AD 696527

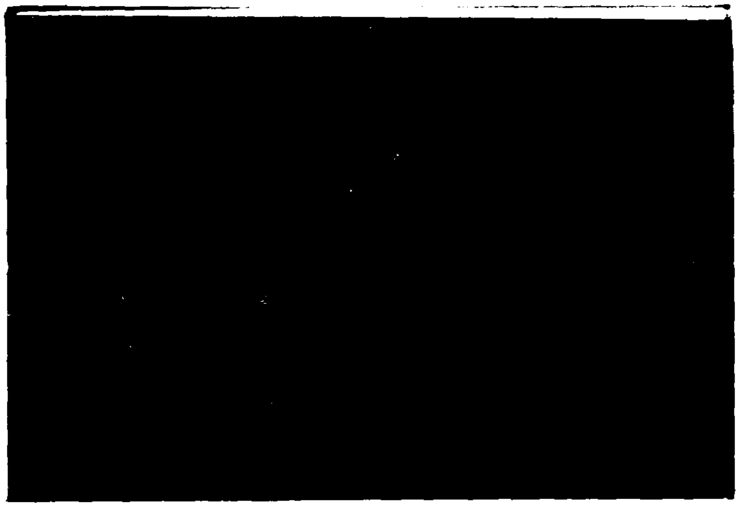

ATMOSPHERIC PHYSICS

School of Physics and Astronomy

UNIVERSITY OF MINNESOTA

46

The Use of Extinction from High Altitude

Balloons as a Probe

of the Atmospheric Aerosols*

by

T. J. Pepin

Atmospheric Physics Report

No. AP-31

October, 1969

*This work was supported by the Office of Naval Research under Contract No. N00014-67-A-0113-0004.

Abstract

A simple instrument is described that measures the intensity of solar radiation in four spectral regions. Instruments of this type have been used to observe the atmospheric extinction from high altitude balloons at sunrise since mid 1965. The data from these balloon flights are described and the vertical profiles of atmospheric aerosols determined from these measurements are presented. Evidence is given for the time variation of aerosols at high altitude.

I. Introduction

In the past decade a number of vertical soundings using balloon borne collecting devices and sampling devices have been made to determine the vertical distribution, concentration and composition of the atmospheric aerosols. Also, indirect measurements have been made of the aerosols in the stratosphere using optical techniques, e.g. twilight sky intensity measurements, searchlight and laser probing and solar extinction measurements from rockets and satellites. From these measurements it has long been realized that the concentration of the aerosols varies in time. Because of the complexity of the collecting and sampling devices and the difficulty of reliably observing the stratospheric aerosols from the surface, it has been difficult to monitor the time variations of this important atmospheric constituent.

A small simple optical instrument was developed that measures the extinction of the solar radiation at four wavelengths from a high altitude balloon. From these measurements using the techniques described in this paper, the vertical concentration times the effective scattering size of the aerosols can easily be determined. Since the instrument is small and weighs less than 12 pounds it can routinely be carried to high altitudes on 100,000 ft^3 balloons enabling the study of the time variations of the aerosols.

II. Description of Equipment and Measurement.

The balloon borne instrument consists of four telescopes that look in the horizontal direction with 14 degree x 14 degree fields each centered 90 degrees in azimuth from each other. This assembly is rotated beneath the balloon at a constant angular speed of approximately 1 revolution per minute as the balloon floats at constant altitude. During this time the rising sun traverses the vertical fields of the telescopes. The intensity of the solar radiation is measured in four spectral regions as a function of time by the telescopes as

they rotate. The intensities are measured to an accuracy of 1%.

The construction details of these telescopes are illustrated in Figure 1. For convenience the telescopes will be referred to as A, B, C and D for the remainder of this report. Table 1 summarizes the spectral sensitivities of the telescopes.

Table 1

Telescope	λ[°A]	Δλ [°A]
A	3670	300
B	4300	350
C	5950	400
D	9100	1400

(λ is wavelength of maximum sensitivity and Δλ is the full width at one half max sensitivity.)

Telescopes A, B and C employ type 929 vacuum phototubes with S-4 response as detectors. Telescope D uses a type 925 vacuum phototube which has a S-1 response. For each telescope the vignetting curve is measured by scanning over the sun before each flight. This allows one to make a correction for any deviation from a flat response across the field. This correction is less than 4%.

Figure 2 illustrates the exponential extinction coefficient per atmosphere (k) as a function of wavelength produced by the various atmospheric absorbers under good average conditions at sea level. There are three curves illustrated in this figure, one for the molecular or Rayleigh component per atmosphere ($k \propto 1/\lambda^4$), one for the aerosol component per atmosphere (this curve assumes $k \propto 1/\lambda$ and is normalized to C. W. Allen's (1963) value at 1μ) and the third curve illustrates the atmospheric absorption for ozone as a function of wavelength assuming 3mm of

ozone per atmosphere. Also marked on this figure are the spectral responses of the four telescopes. One observes that telescope A is primarily sensitive to the extinction produced by the molecular or Rayleigh scattering of the atmosphere. Telescope B is also sensitive to the Rayleigh component and to some extent the extinction produced by the atmospheric aerosols. Telescope C is centered in the middle of the Chappuis bands of ozone. Along with being sensitive to extinction produced by the molecular and aerosol components of the atmosphere it is sensitive to absorption caused by the Chappuis bands. Telescope D is primarily sensitive to the extinction caused in the atmosphere due to the presence of the atmospheric aerosol component.

Figure 3 demonstrates the intensity that one would expect to observe as a function of atmospheric path for each of the four telescopes assuming a pure molecular atmosphere.

From the flight of April 12, 1967 Figure 4 has been constructed by plotting the observed intensity from each of the telescopes as a function of the calculated air mass (air mass calculations will be described in the next section). One observes the similarity of the data from telescopes A and B to that expected for a Rayleigh atmosphere whereas the data of telescopes C and D appear different. The difference in the data of telescope C from that expected for a Rayleigh atmosphere is a reflection of the extinction produced by the ozone component of the atmosphere. The inflection in the data from telescope D between 5 and 8 atmospheres is produced by an increased concentration of atmospheric aerosols above the tropopause as will be discussed in later sections.

The data from this series of measurements from telescope C will be discussed in a future report as this report will primarily concern itself with the atmospheric aerosols.

III. Calculation of Air Mass.

In order to plot the telescope data as a function of air mass, one must calculate the atmospheric air mass traversed by the solar ray before it enters the telescope.

A knowledge of the position of the balloon as a function of time, which is determined from the pressure measured using an Olland cycle on the balloon and from tracking the balloon using a G.M.D., enables one to determine by the use of the Air Almanac the true elevation angle (α) of the sun as a function of time. The air mass can then be calculated knowing the elevation angle of the sun and the geometric altitude of the balloon (h_B). The geometry of the calculation is illustrated in Figure 5. α is negative for elevation angles below the horizontal direction.

Considering first positive elevation angles, the air mass traversed by a solar ray before entering the telescope at altitude of h_B when the sun is at elevation angle α is given by:

$$A(\alpha,h_B) = A(\alpha,0)\,\frac{P(h_B)}{P(0)}\;,\ \text{for}\ \alpha \geq 0 \qquad (1)$$

where P(h) is the pressure at altitude h and $A(\alpha,0)$ is the number of air masses from the surface at elevation angle α without the correction for refraction. Since the refraction at positive elevation angles is proportional to the density at the balloon's altitude, the correction for refraction does not significantly influence relation(1) and need not be considered for positive elevation angles. The surface air mass $A(\alpha,0)$ has been measured and calculated for various model atmospheres by a number of authors. (A good review of the determination of $A(\alpha,0)$ has been presented by Rozenberg (1966)). For the present study the author has used the air mass tabulated by Allen (1963).

For negative elevation angles one can calculate the air mass traversed by the solar beam before reaching the telescope by observing that at the tangent height of the ray, h_T, the air mass to the tangent point is given by:

$$A(0,h_T) = A(0,0)\,\frac{P(h_T)}{P(0)} \quad . \qquad (2)$$

But, the total air mass at elevation angle $-\alpha$ is just twice the air mass to the tangent point minus the air mass at $+\alpha$. OR

$$A(-\alpha,h_B) = 2\,A(0,0)\,\frac{P(h_T)}{P(0)} - A(\alpha,0)\,\frac{P(h_B)}{P(0)} \quad . \qquad (3)$$

In relations(2) and (3), h_T is the height of the tangent ray which is affected by refraction. Its height can be calculated by an iterative procedure.

From Figure 5 it may be seen that the tangent height of a ray with no refraction is given by

$$h_T = h_B \cos\alpha - R\,(1-\cos\alpha) \qquad (4)$$

where R is the radius of the earth. From the tangent height for a straight ray (no refraction) the first estimate of the pressure of the true tangent altitude is determined, and thus the first estimate of the air mass (A') to the tangent point traversed by the ray, using equation (2). The refraction of the tangent ray to the tangent point is then calculated as

$$\beta = \beta_o\,A'\,\frac{1}{.965 + .0035\,T(h_T)} \qquad (5)$$

where $T(h_T)$ is the temperature at altitude h_T in degrees centigrade. In equation (5), which is due to C. W. Allen (1963), β_o is the refraction per air

mass and for the wavelengths used in these experiments has the numerical value 1 min of arc per air mass.

Since β is a small angle and most of the refraction occurs near the tangent altitude one may obtain a second estimate of h_T from equation (4) by substituting for α the apparent elevation angle $-\alpha + \beta$.

Having thus calculated the tangent height, corrected for refraction to first order, relation (2) can again be used to calculate the air mass corrected for refraction to first order and then the calculation of the tangent height can be repeated and the iterative procedure can be continued.

A good check on the calculation of the tangent height is offered by the data itself. It is observed that in flights made at times of good weather that the signal of telescope D is first observed at the time when one would just predict the sun had come over the limb of the earth. If one calculates the tangent height at the time the first signal is observed using the above method he finds it is only a fraction of a km indicating the correction for refraction has been applied correctly to first order.

IV. Determination of $N\sigma(h)$ from Extinction Data.

The number density times the effective scattering size of the atmospheric aerosols as a function of altitude, $N\sigma(h)$, can be determined from the extinction data from telescope D by considering a model atmosphere consisting of a number of layers and working out the extinction produced in each of the layers as the solar rays traverse them.

The atmosphere below the balloon is conveniently divided into a number of layers by the tangent heights of the observed rays when the sun is below the horizon. It is convenient to index the layers from the balloon down from 1 to k and assign the index 0 to the layer above the balloon of thickness S which is

assumed to contain the aerosols above the balloon. The tangent height, h_k, can be calculated by the method outlined in the previous section and the geometry is illustrated in Figure 6. The path lengths P_{jk} of the jth ray in the kth layer can be calculated from simple geometry and it is found:

$$P_{oo} = [S \{S + 2 (h_o + R) \}]^{1/2} \tag{6}$$

where R is the radius of the earth,

$$P_{jo} = [(h_o + S - h_j) (h_o + S + h_j + 2R)]^{1/2} \tag{7}$$

$$- [(h_o - h_j) (h_o + h_j + 2R)]^{1/2}$$

and for k > 0

$$P_{jk} = 2 [(h_{k-1} - h_j) (h_{k-1} + h_j + 2R)]^{1/2} - \sum_{\substack{i=k+1 \\ i \neq j}}^{j} P_{ji} \, . \tag{8}$$

Invoking the Lambert-Beer law one has the intensity I of the light ray after traversing a path length P when the incident intensity is I' as:

$$I = I' e^{-N \sigma P} \tag{9}$$

where N is the number of scattering centers per cubic volume and σ is the effective cross-section of the average scattering center.

By plotting the observed intensity from telescope D corrected for the Rayleigh component as a function of air mass one can extrapolate to find the intensity at the top of the atmosphere, $I_{\odot}$, and with the observed intensity corrected for the Rayleigh component in the horizontal direction, I_o, one can invert relation (9) to find

$$(N\sigma)_o = \frac{\log_e \frac{I_{\odot}}{I_o}}{P_{oo}}$$

by using relation (6) to calculate P_{oo}.

Having determined $(N\sigma)_o$, one can trace the first ray below the horizontal through the atmosphere, again using relation (9) along with (7) and (8) to find

$$(N\sigma)_1 = \frac{\log_e \frac{I_{\odot}}{I_1} - (N\sigma)_o\, P_{10}}{P_{11}} \quad .$$

One can continue to solve for the $(N\sigma)_k$'s using the measured intensities corrected for the Rayleigh component, I_k, for successive lower layers and in general one finds

$$(N\sigma)_k = \frac{\log_e \frac{I_{\odot}}{I_k} - \sum_{i=0}^{k-1} (N\sigma)_i\, P_{ki}}{P_{kk}}$$

In order to carry out the above calculation one must, as has been pointed out, assume a value for S. In the present work S was first assumed to be the atmospheric scale height and then after the calculation was completed the assumption was made that σ was independent of altitude and the scale height of

the aerosols was determined. This scale height was then used for S and the calculation repeated. Since a balloon at an altitude of 32 km is above almost all of the aerosols the choice of S does not critically influence the results.

As a test of the consistency of this method in one of the balloon flights of this series telescope C was replaced with a telescope D so that there were two identical telescopes looking in the infrared wavelength on the same flight. The data from these telescopes were analyzed independently and are plotted in Figure 7. Both are seen to give the same result.

V. Data from Extinction Flights.

From the summer of 1965 to early 1968 a number of extinction flights were made from Minneapolis and one flight (774) was made from the Panama Canal Zone.

The data from these flights have been analyzed using the method outlined in the above sections and $N\sigma(h)$ has been determined at the time of each of the measurements. Figures 8 through 29 illustrate the $N\sigma(h)$'s determined in these measurements. In these figures the $(N\sigma)_k$'s have been plotted vs. the tangent height h_k for the k th layer. The curved grid lines on the background of these figures are proportional to lines of constant mixing ratios for the atmospheric aerosols if the effective scattering cross-section is independent of altitude. The numerical values on the lines, thus interpreted, are proportional to the mixing ratio.

In this series of flights the highest concentration of aerosols above the tropopause at Minneapolis was observed in Flight 780 on December 30, 1966. The observed $N\sigma$ in this layer was 6×10^{-8} cm^{-1}. If one assumes the average radius of the aerosols responsible for the extinction was $.5\mu$, one calculates the concentration of aerosols in this layer to be $4/cm^3$.

In Flight 774 from Panama a high $N\alpha\ (> 6 \times 10^{-8}\ cm^{-1})$ was observed in the stratosphere of the tropical atmosphere. This flight was made of the same time that J. M. Rosen (1968) made direct soundings of the aerosols. He too found a high concentration of aerosols at this time above Panama.

VI. Variability of the Stratospheric Aerosols.

Study of these figures reveals the variability of the aerosol concentration in the stratosphere and at an altitude just above the tropopause. These variations are in fact systematic in time as is evidenced in Figure 30. In this figure the extinction coefficient k_{IR}, determined from the data of the D telescope when the solar ray traversed one atmospheric air mass, is plotted above the date of each flight. As has been pointed out in earlier sections, k_{IR}, the extinction coef., is proportional to the average concentration of aerosols along the path. The tangent height of a path through the atmosphere that traverses 1 air mass is about 26 km.

VII. Acknowledgments

The author would like to thank Dr. F. Gillett for his help in the early development of the instrument and Mr. N. Kjome and Mr. R. Maas for their assistance in preparing the equipment and helping with the balloon flights.

The stimulating discussions with Drs. H. Mantis and J. Rosen and the valuable advice of Dr. E. P. Ney greatly furthered this research.

References

1. Allen, C. W.: 1963, Astrophysical Quantities, Athlone Press.

2. Rosen, J. M. : 1964, J. Geophys. Res. 69, 4673.

3. Rosen, J. M. : 1968, J. Geophys. Res. 73, 479.

4. Rosen, J. M. : 1969, Space Science Rev. 9, 58.

5. Rozenberg, G. V., 1966, Twilight, Plenum Press.

Figures:

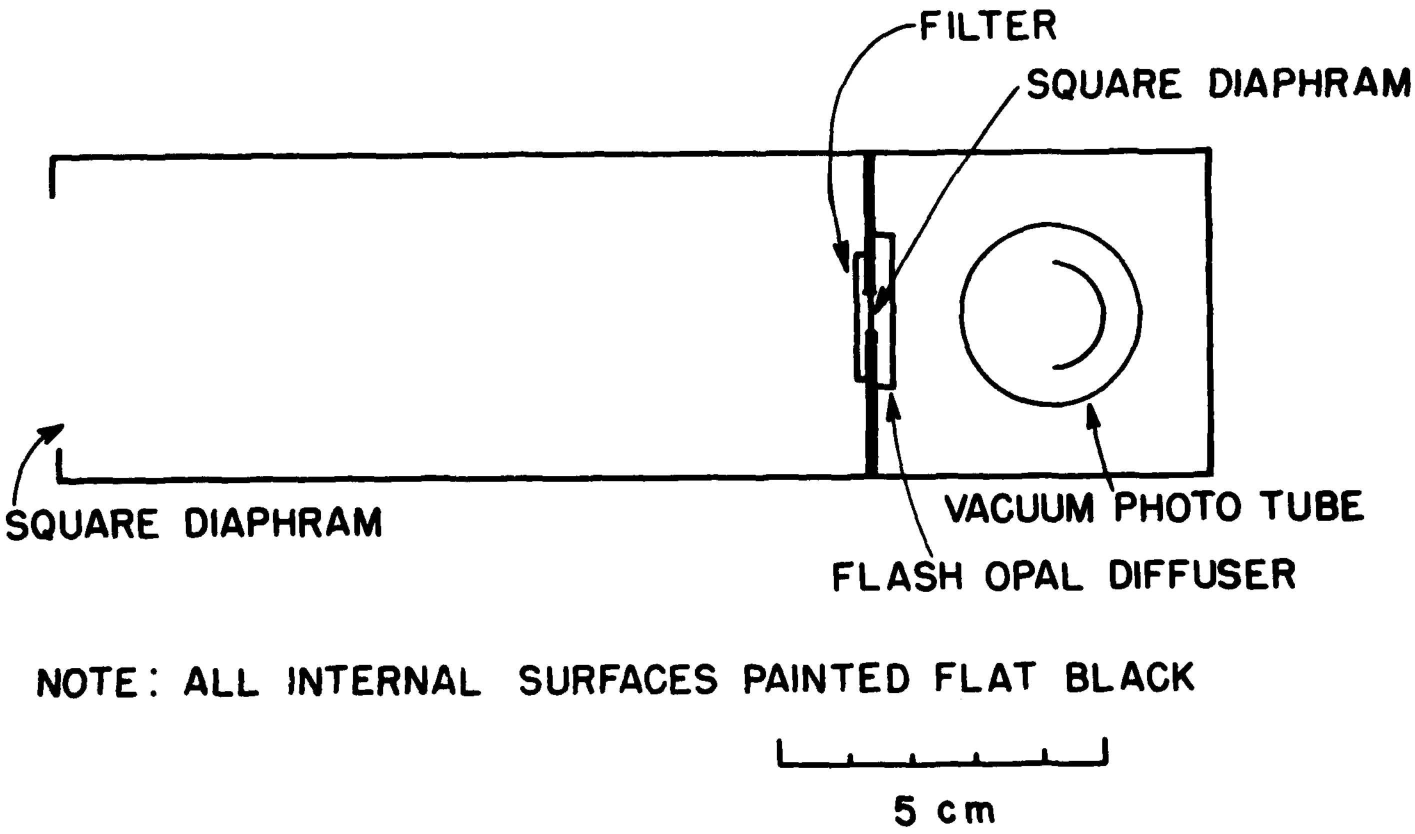
FILTER
SQUARE DIAPHRAM
SQUARE DIAPHRAM
VACUUM PHOTO TUBE
FLASH OPAL DIFFUSER
NOTE: ALL INTERNAL SURFACES PAINTED FLAT BLACK
5 cm

Figure 1

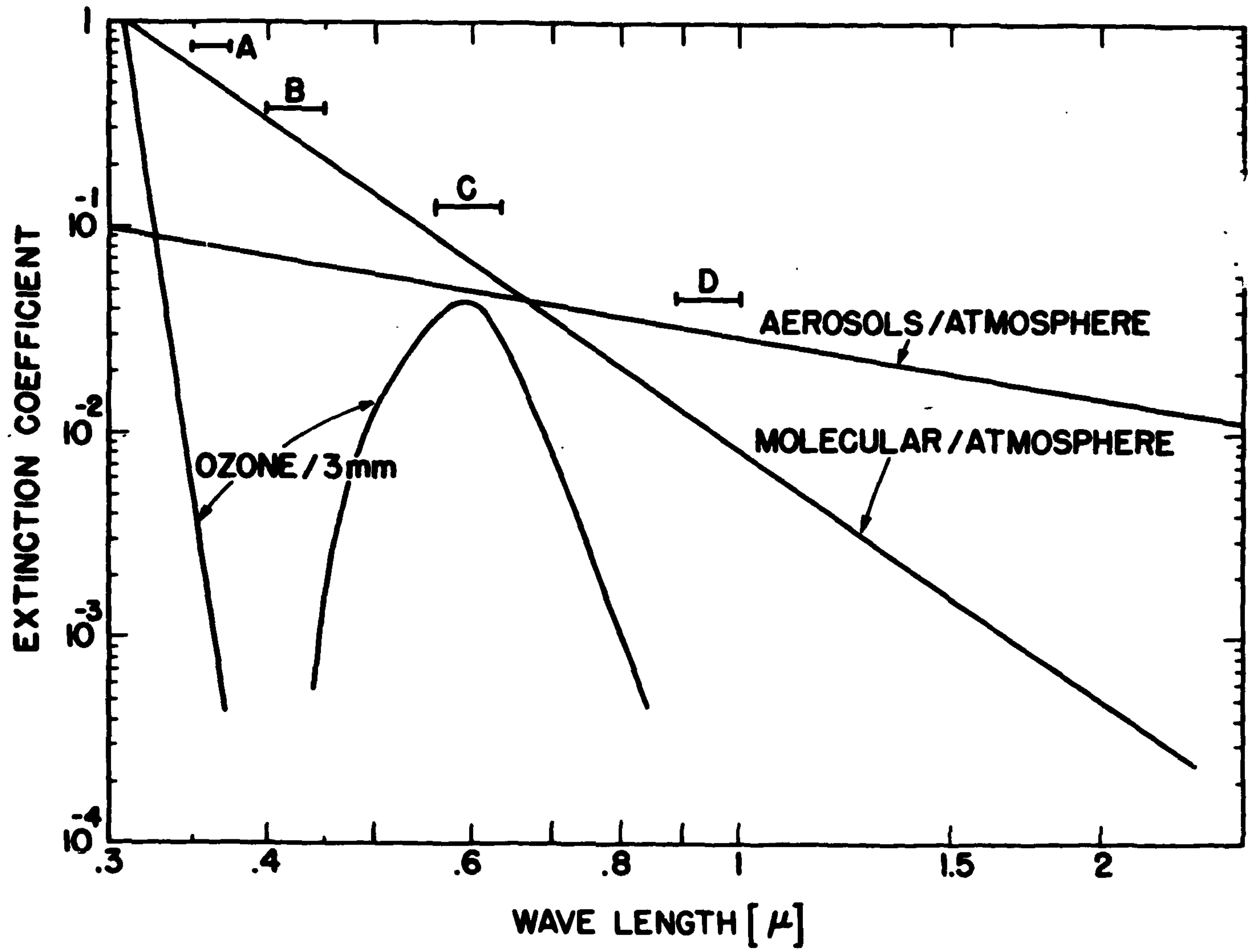

A
B
C
D
AEROSOLS / ATMOSPHERE
MOLECULAR / ATMOSPHERE
OZONE / 3mm
EXTINCTION COEFFICIENT
1
10^{-1}
10^{-2}
10^{-3}
10^{-4}
.3
.4
.6
.8
1
1.5
2
WAVE LENGTH [μ]

Figure 2

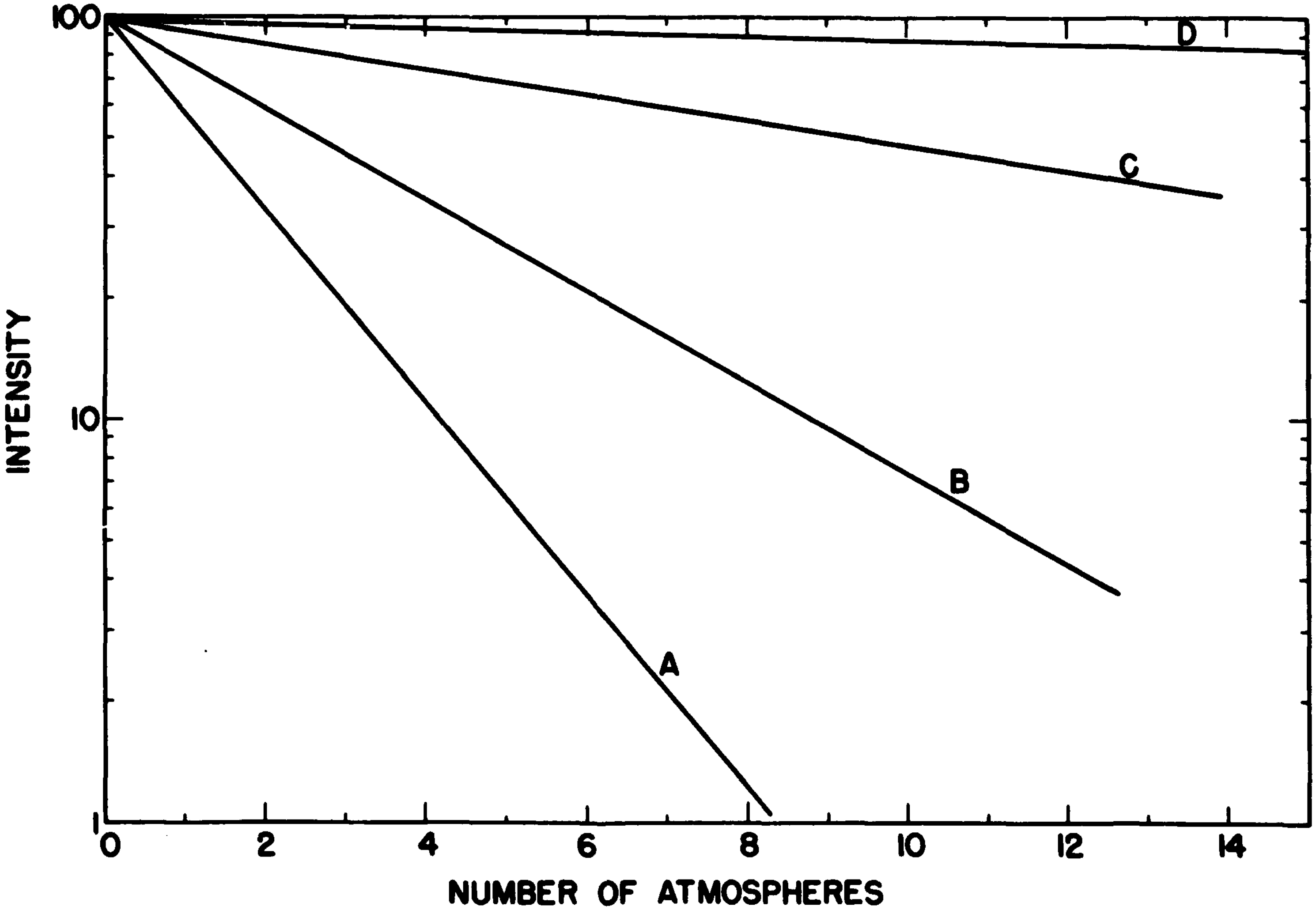

Figure 3

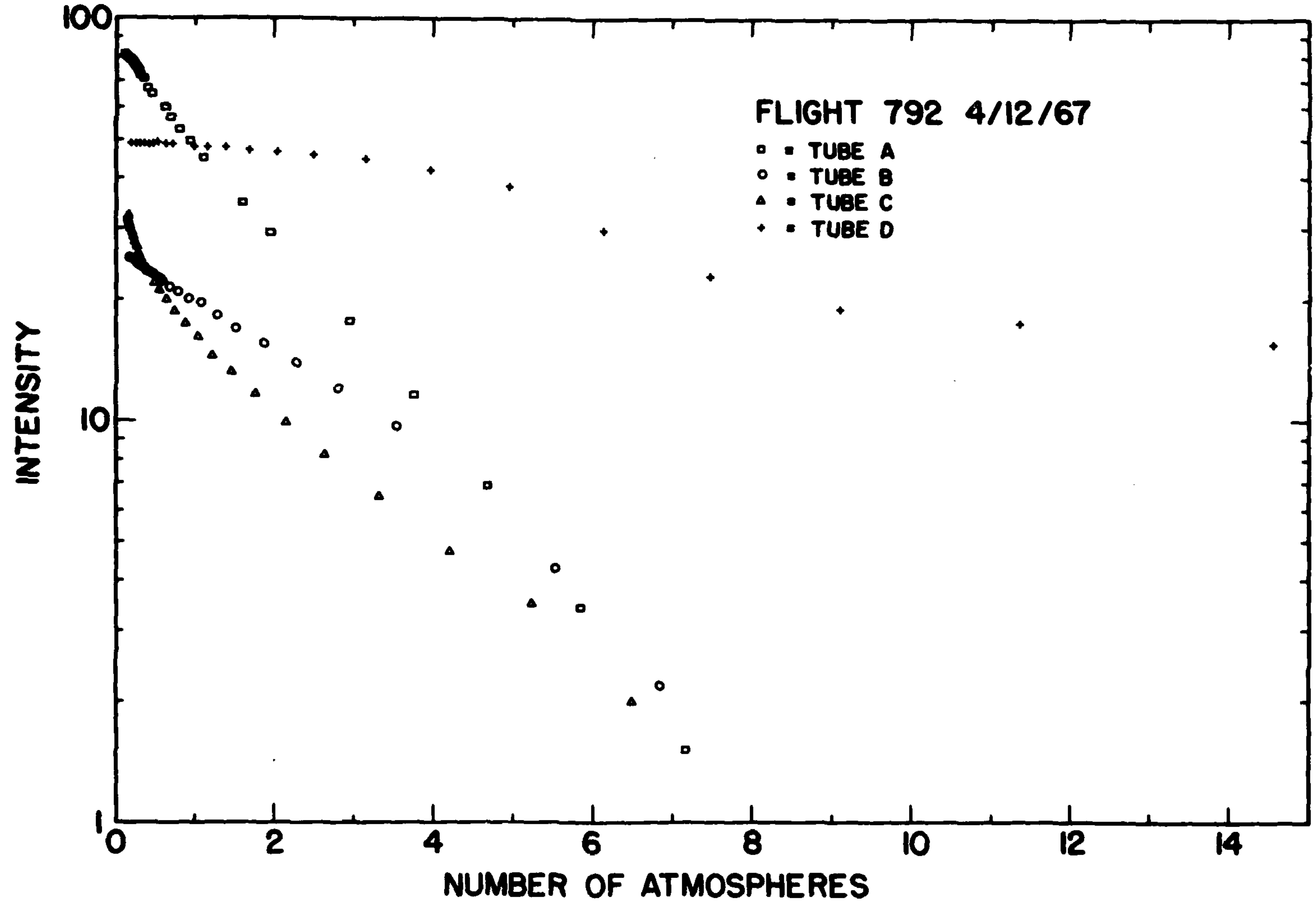

100
10
1
INTENSITY
0
2
4
6
8
10
12
14
NUMBER OF ATMOSPHERES
FLIGHT 792 4/12/67
▫ = TUBE A
○ = TUBE B
△ = TUBE C
+ = TUBE D

Figure 4

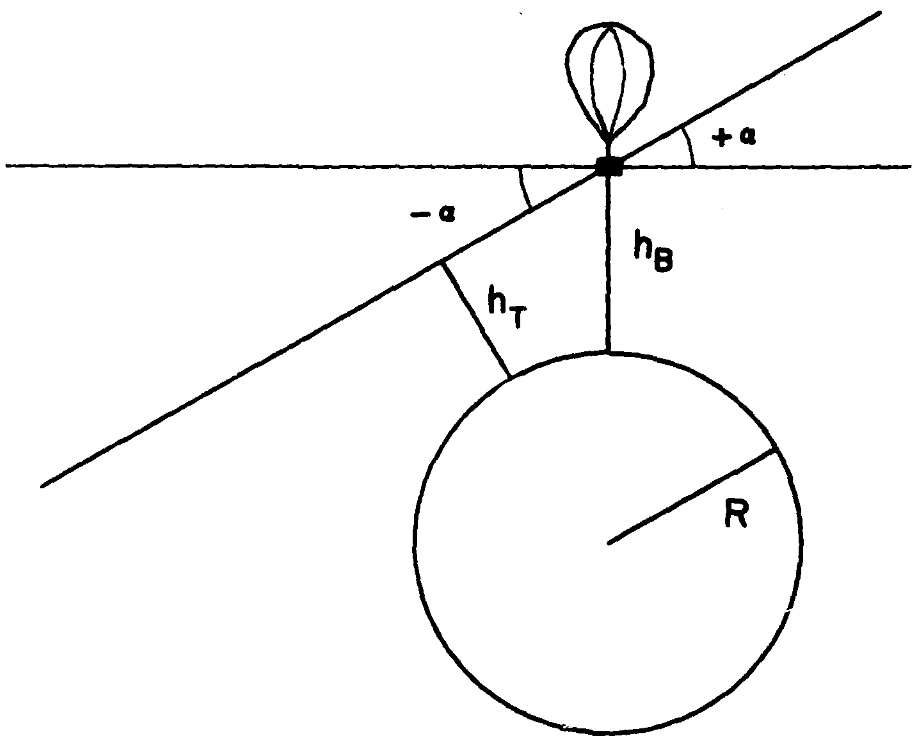

Figure 5

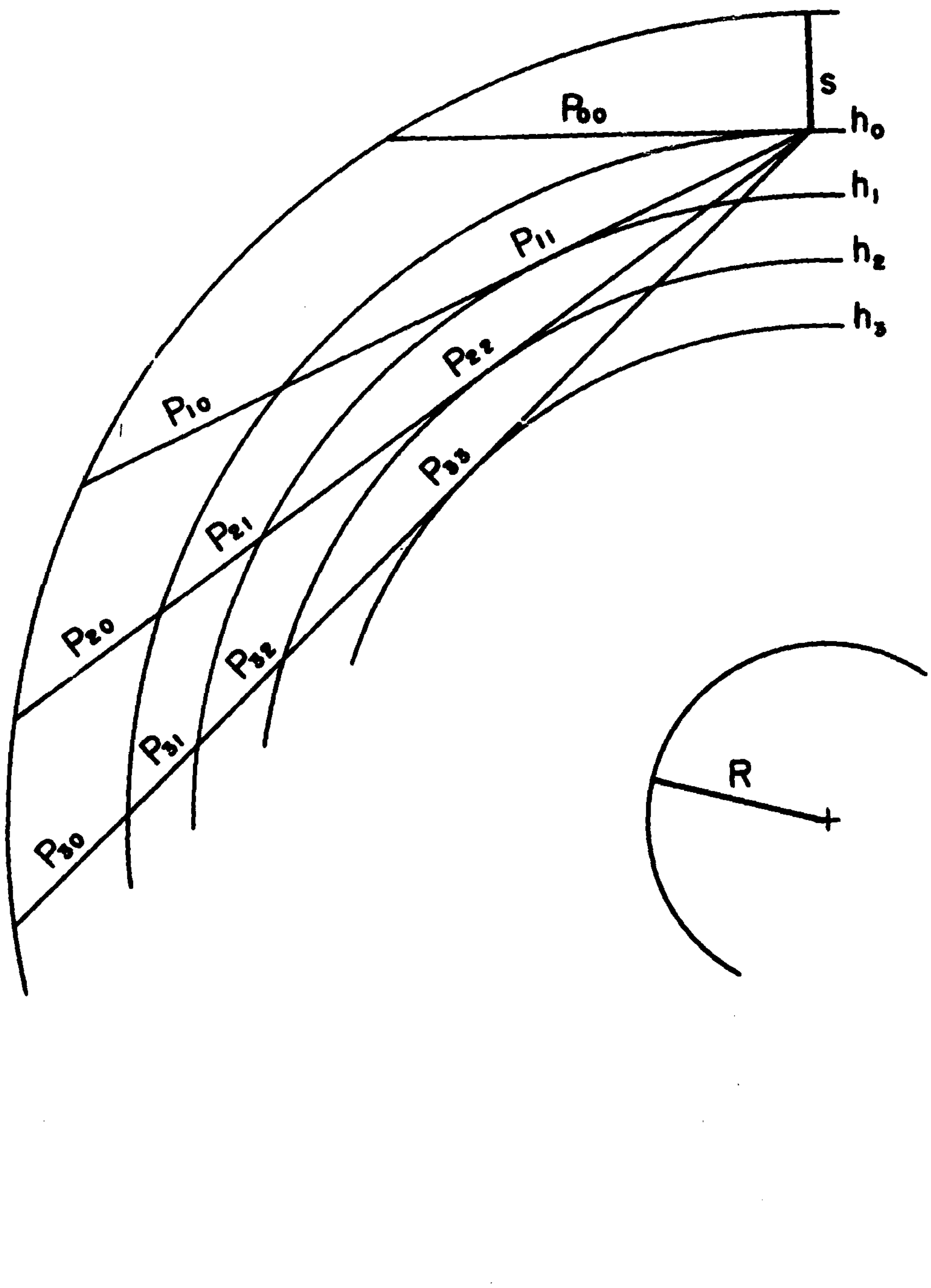

Figure 6

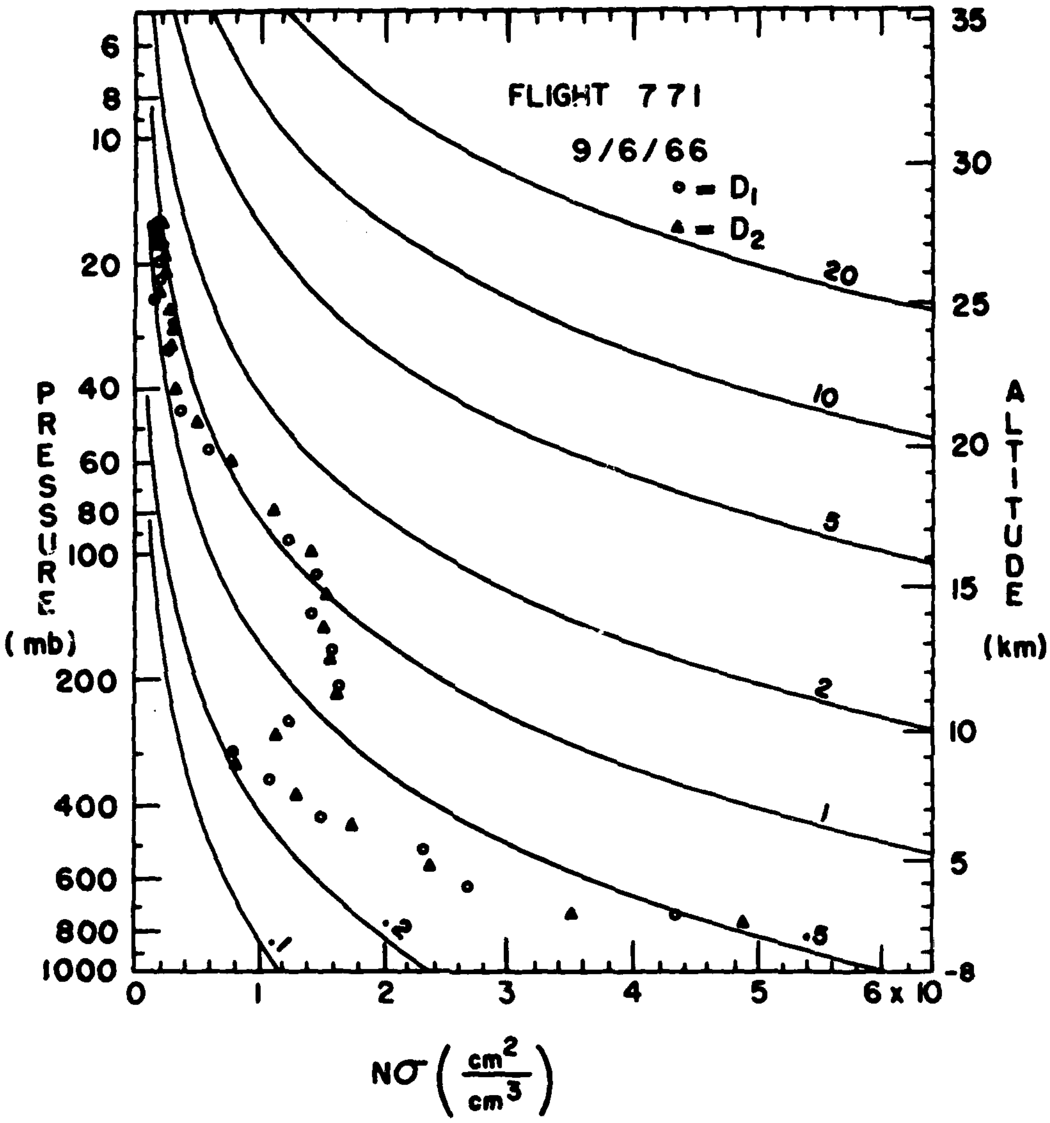

FLIGHT 771
9/6/66
○ = D_1
▲ = D_2
PRESSURE (mb)
ALTITUDE (km)
$N\sigma\left(\frac{cm^2}{cm^3}\right)$
6 x 10

Figure 7

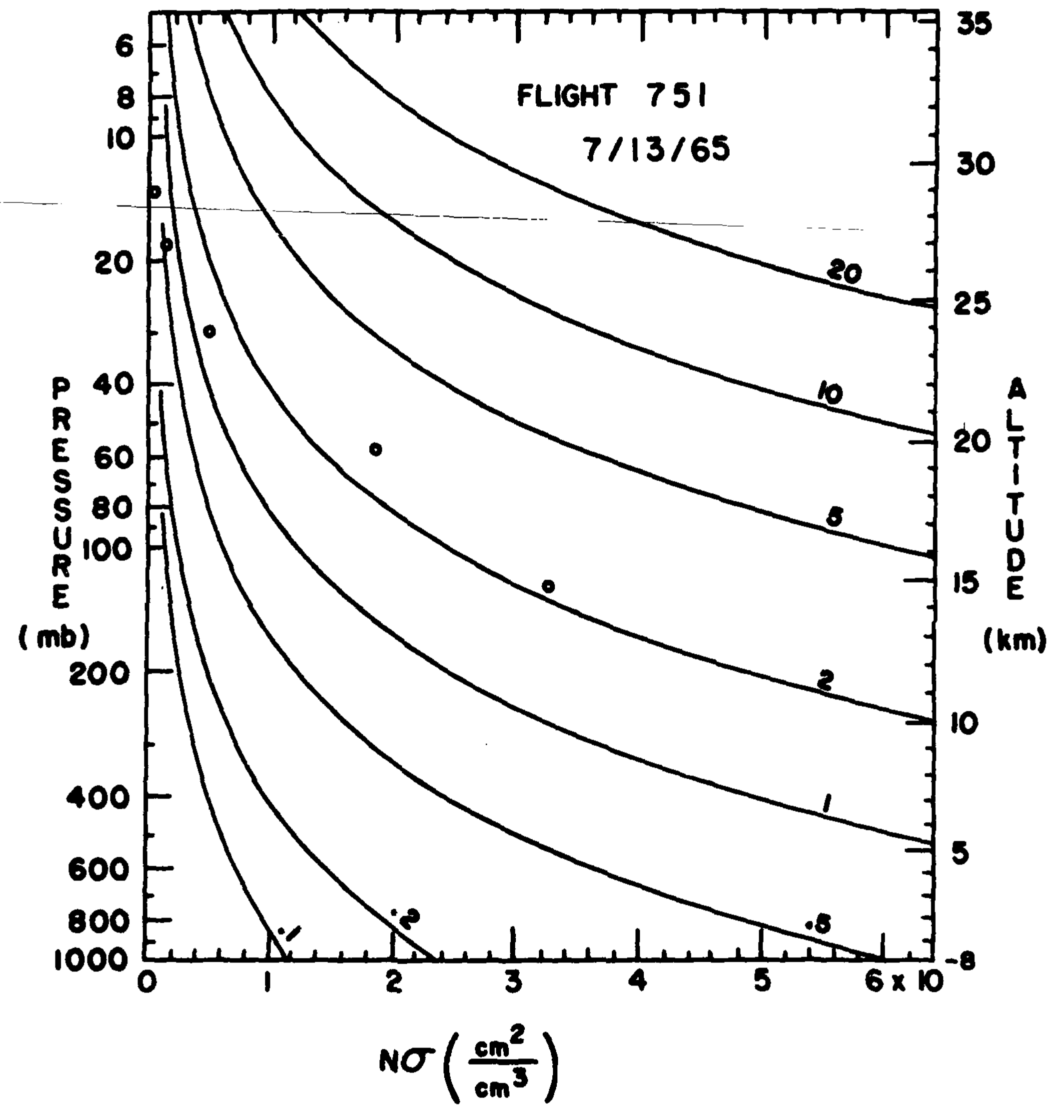
FLIGHT 751
7/13/65
PRESSURE (mb)
ALTITUDE (km)
6
8
10
20
40
60
80
100
200
400
600
800
1000
35
30
25
20
15
10
5
-8
0
1
2
3
4
5
6 x 10
20
10
5
2
1
.5
.2
.1
$N\sigma\left(\frac{cm^2}{cm^3}\right)$

Figure 8

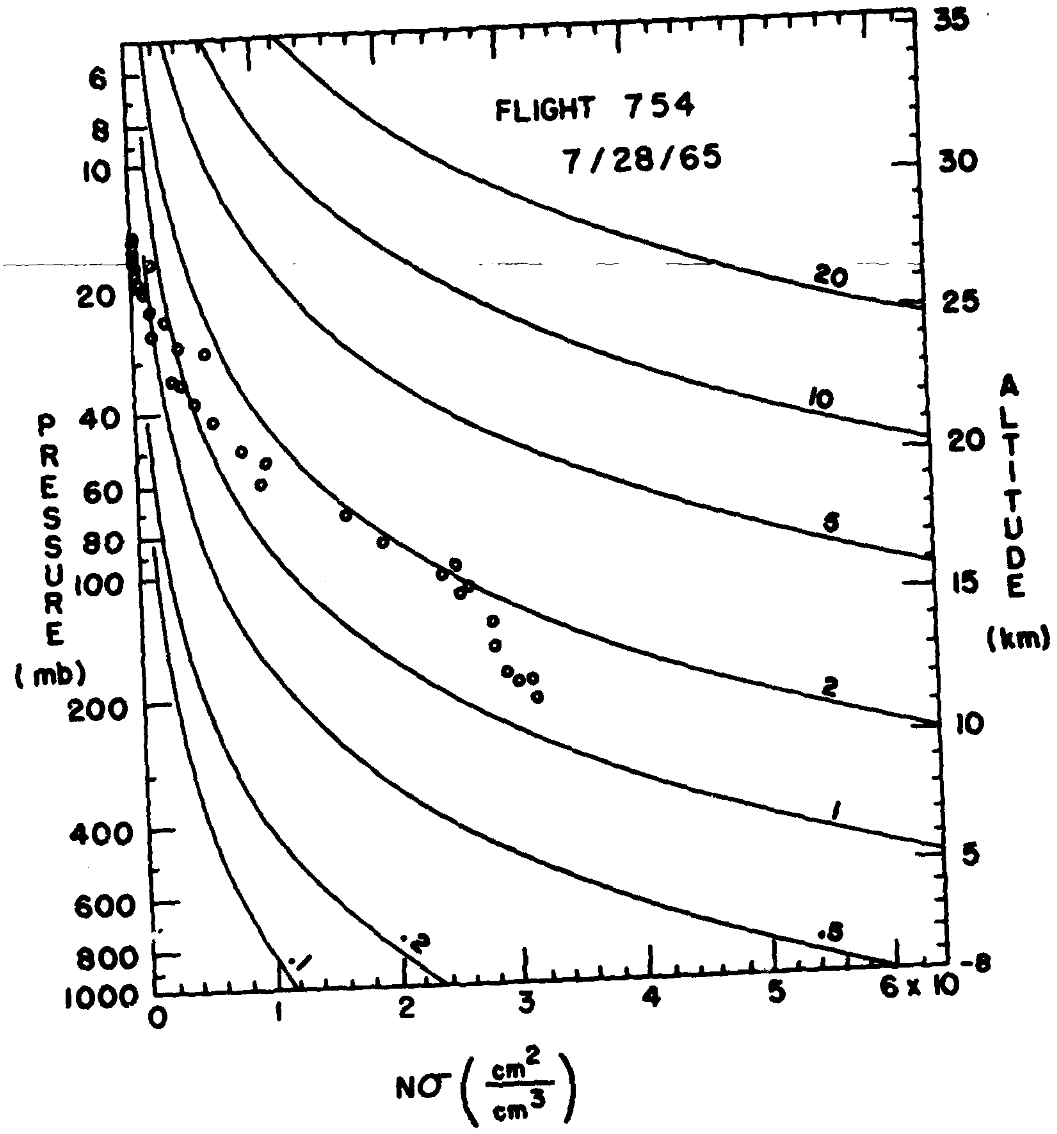
FLIGHT 754
7/28/65
PRESSURE (mb)
ALTITUDE (km)
20
10
5
2
1
.5
.2
.1
6
8
10
20
40
60
80
100
200
400
600
800
1000
35
30
25
20
15
10
5
0
1
2
3
4
5
6 x 10
-8
$N\sigma\left(\frac{cm^2}{cm^3}\right)$

Figure 9

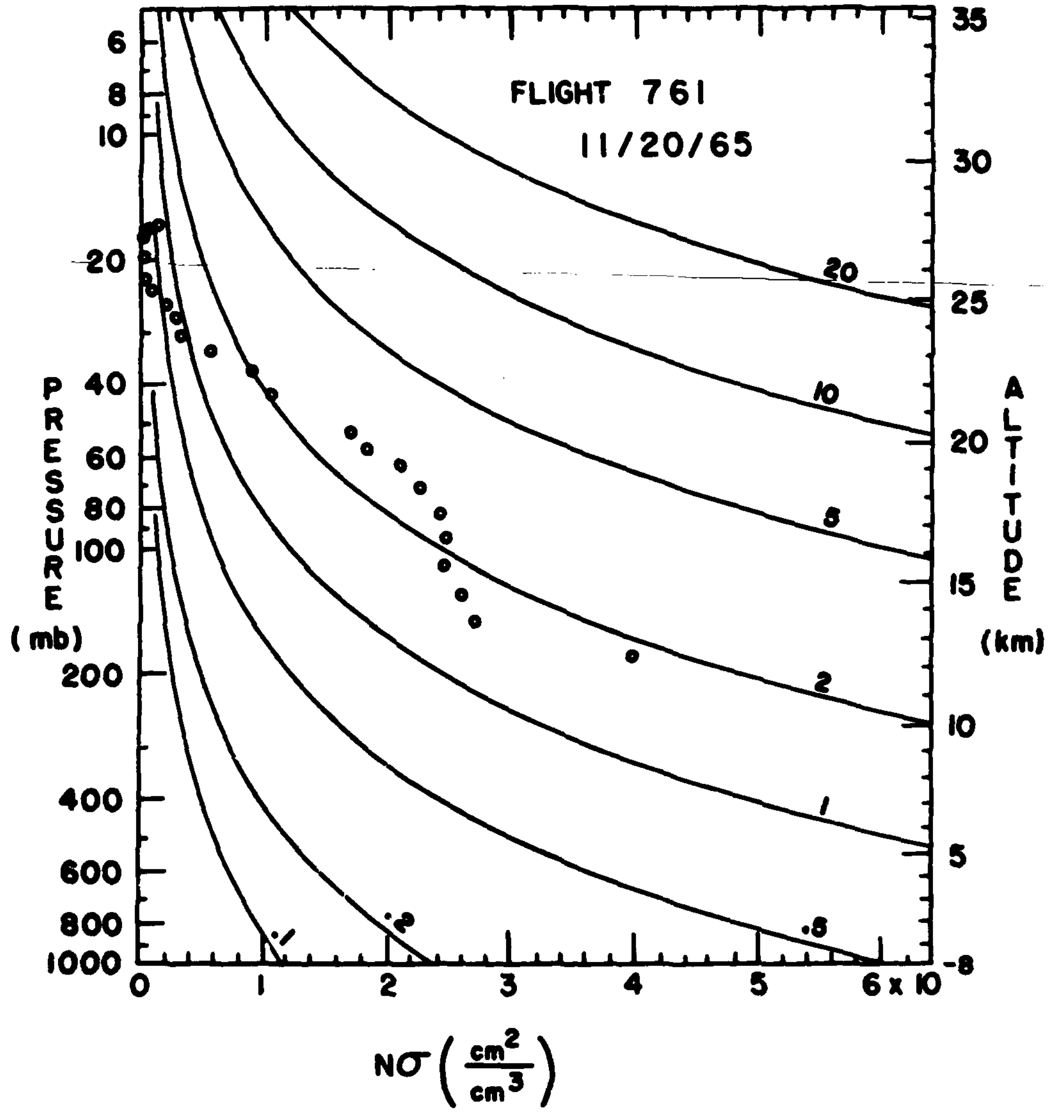

FLIGHT 761
11/20/65
PRESSURE (mb)
ALTITUDE (km)
6
8
10
20
40
60
80
100
200
400
600
800
1000
35
30
25
20
15
10
5
-8
0
1
2
3
4
5
6 x 10
20
10
5
2
1
.5
.2
.1
$N\sigma\left(\frac{cm^2}{cm^3}\right)$

Figure 10

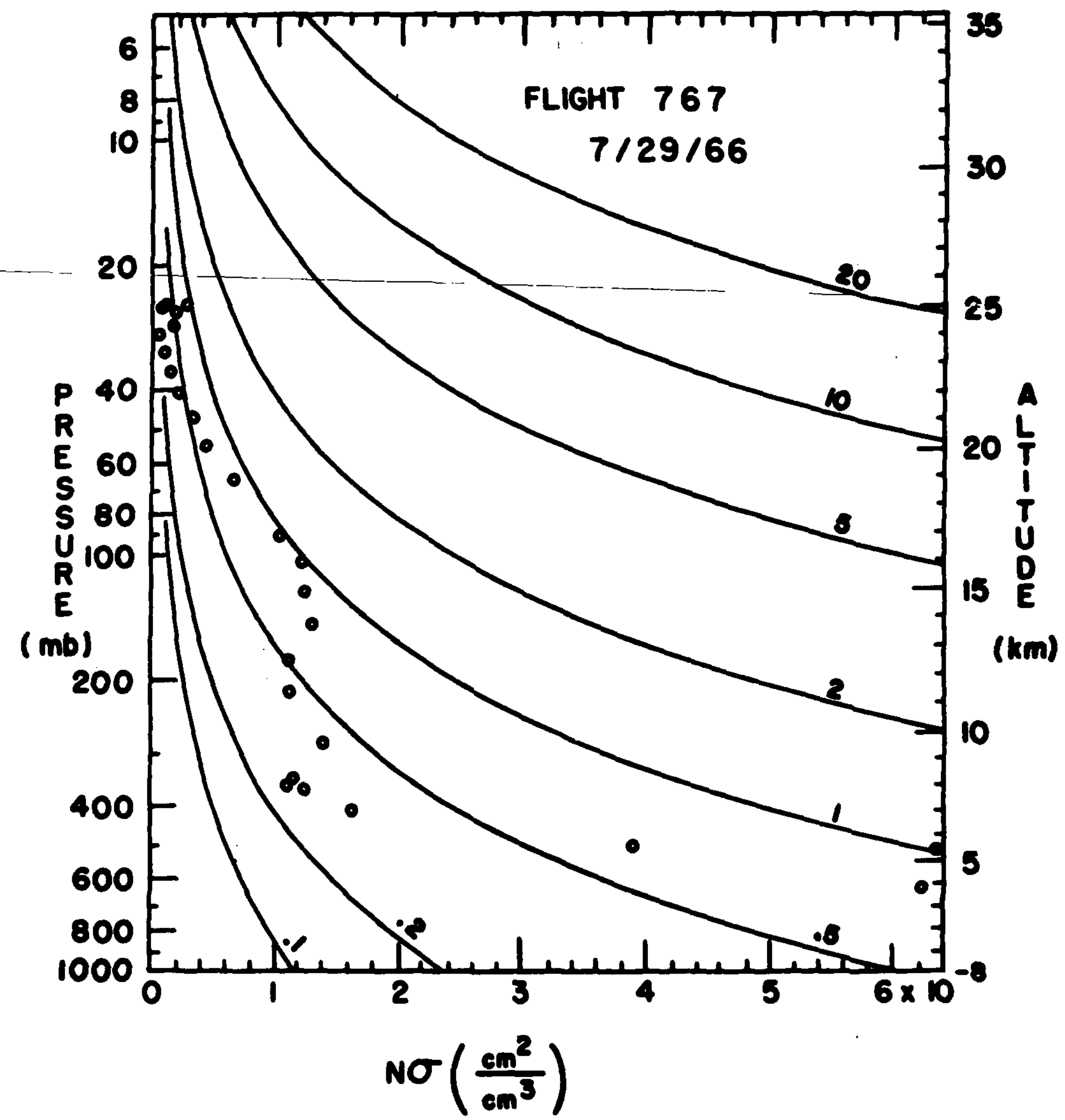
FLIGHT 767
7/29/66
PRESSURE (mb)
ALTITUDE (km)
6
8
10
20
40
60
80
100
200
400
600
800
1000
35
30
25
20
15
10
5
-8
0
1
2
3
4
5
6 x 10
20
10
5
2
1
.5
.2
.1
$N\sigma \left(\frac{cm^2}{cm^3}\right)$

Figure 11

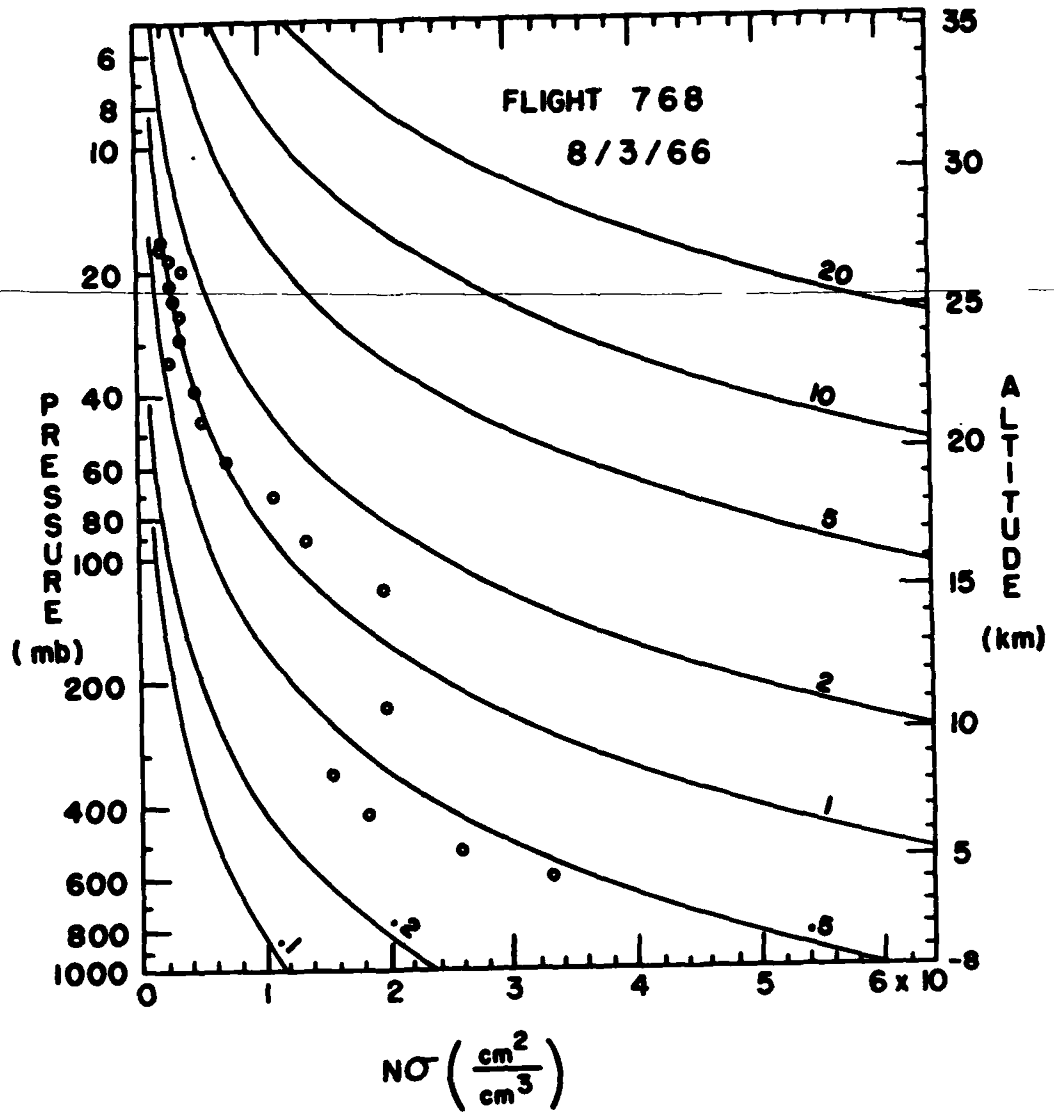

FLIGHT 768
8/3/66
PRESSURE (mb)
ALTITUDE (km)
6
8
10
20
40
60
80
100
200
400
600
800
1000
35
30
25
20
15
10
5
20
10
5
2
1
.5
.2
.1
0
1
2
3
4
5
6 x 10^-8
NO (cm^2 / cm^3)

Figure 12

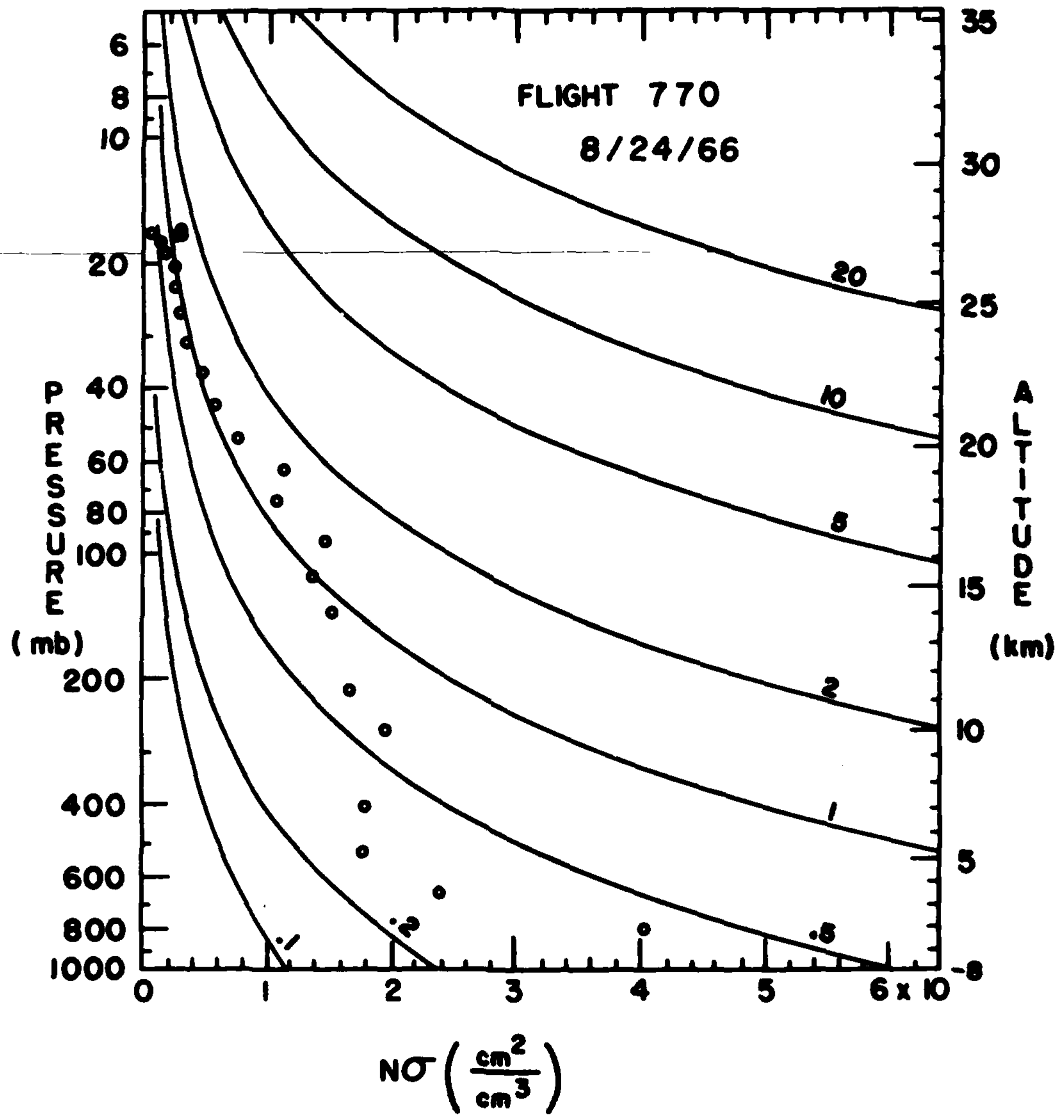

FLIGHT 770
8/24/66
PRESSURE (mb)
6
8
10
20
40
60
80
100
200
400
600
800
1000
ALTITUDE (km)
35
30
25
20
15
10
5
0
1
2
3
4
5
6 x 10
-8
20
10
5
2
1
.5
.2
.1
$N\sigma\left(\frac{cm^2}{cm^3}\right)$

Figure 13

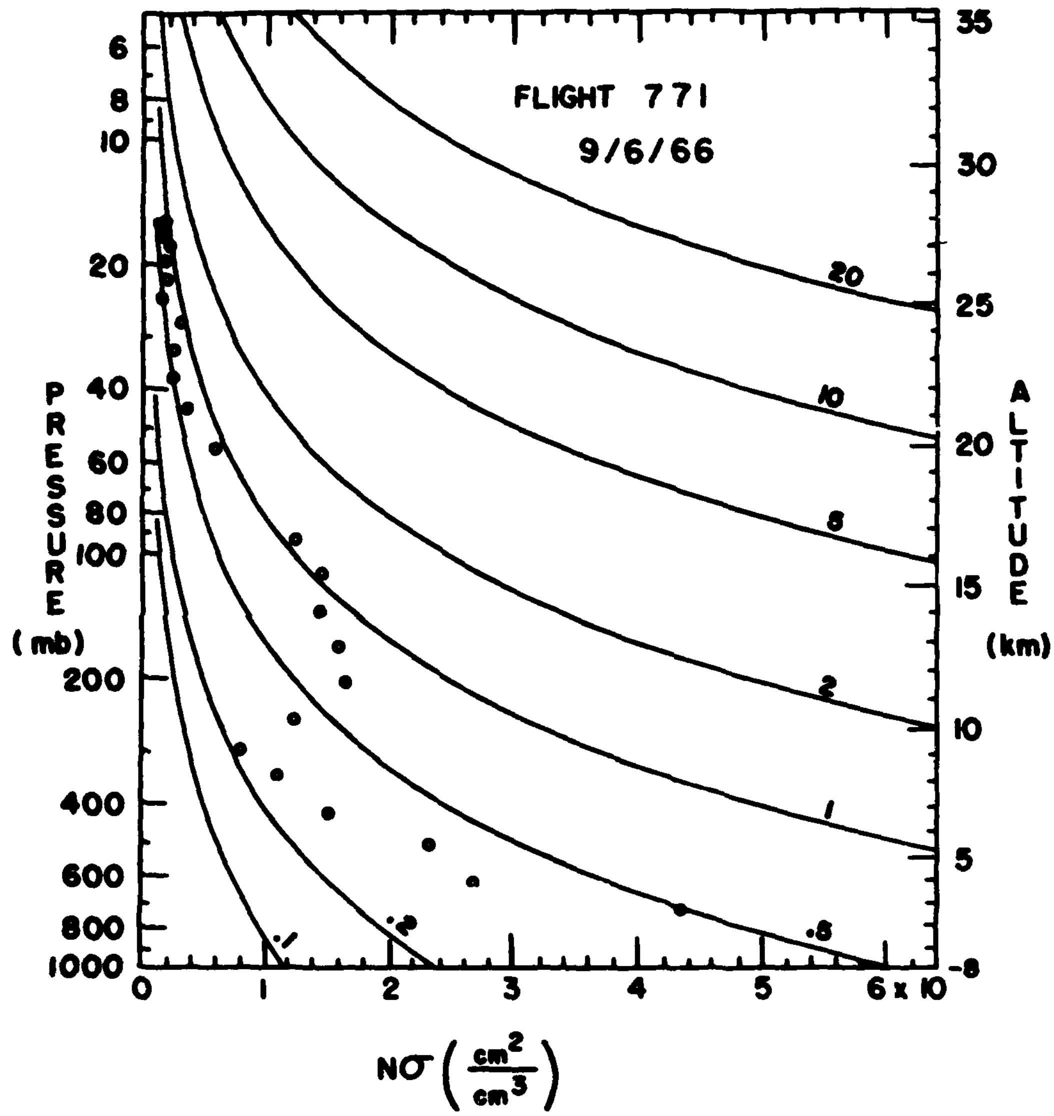

FLIGHT 771
9/6/66
PRESSURE (mb)
ALTITUDE (km)
6
8
10
20
40
60
80
100
200
400
600
800
1000
35
30
25
20
15
10
5
-8
20
10
5
2
1
.5
.2
.1
0
1
2
3
4
5
6 x 10
$N\sigma\left(\frac{cm^2}{cm^3}\right)$

Figure 14

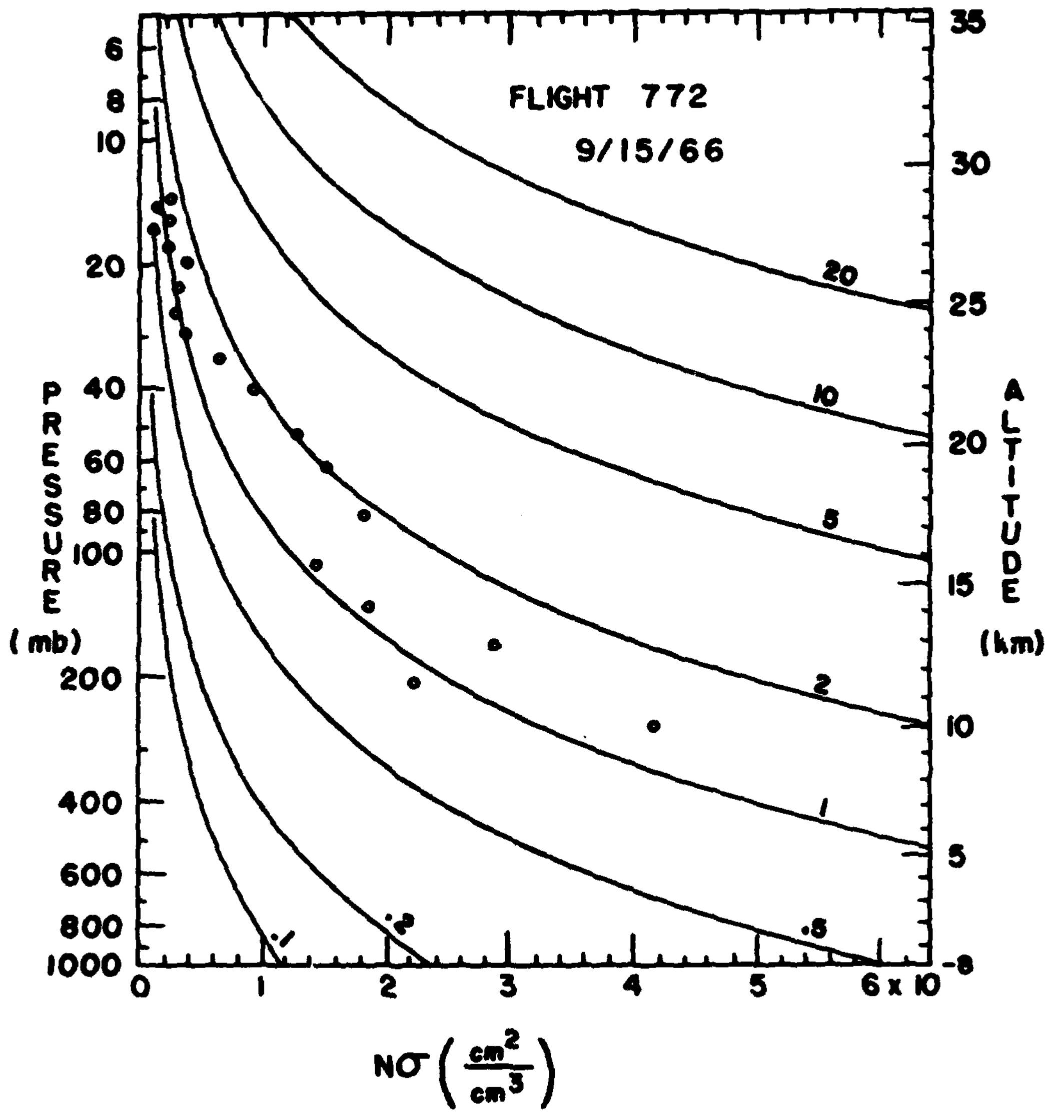
FLIGHT 772
9/15/66
PRESSURE (mb)
ALTITUDE (km)
$N\sigma \left(\frac{cm^2}{cm^3} \right)$
6 x 10^-8
20
10
5
2
1
.5
.2
.1

Figure 15

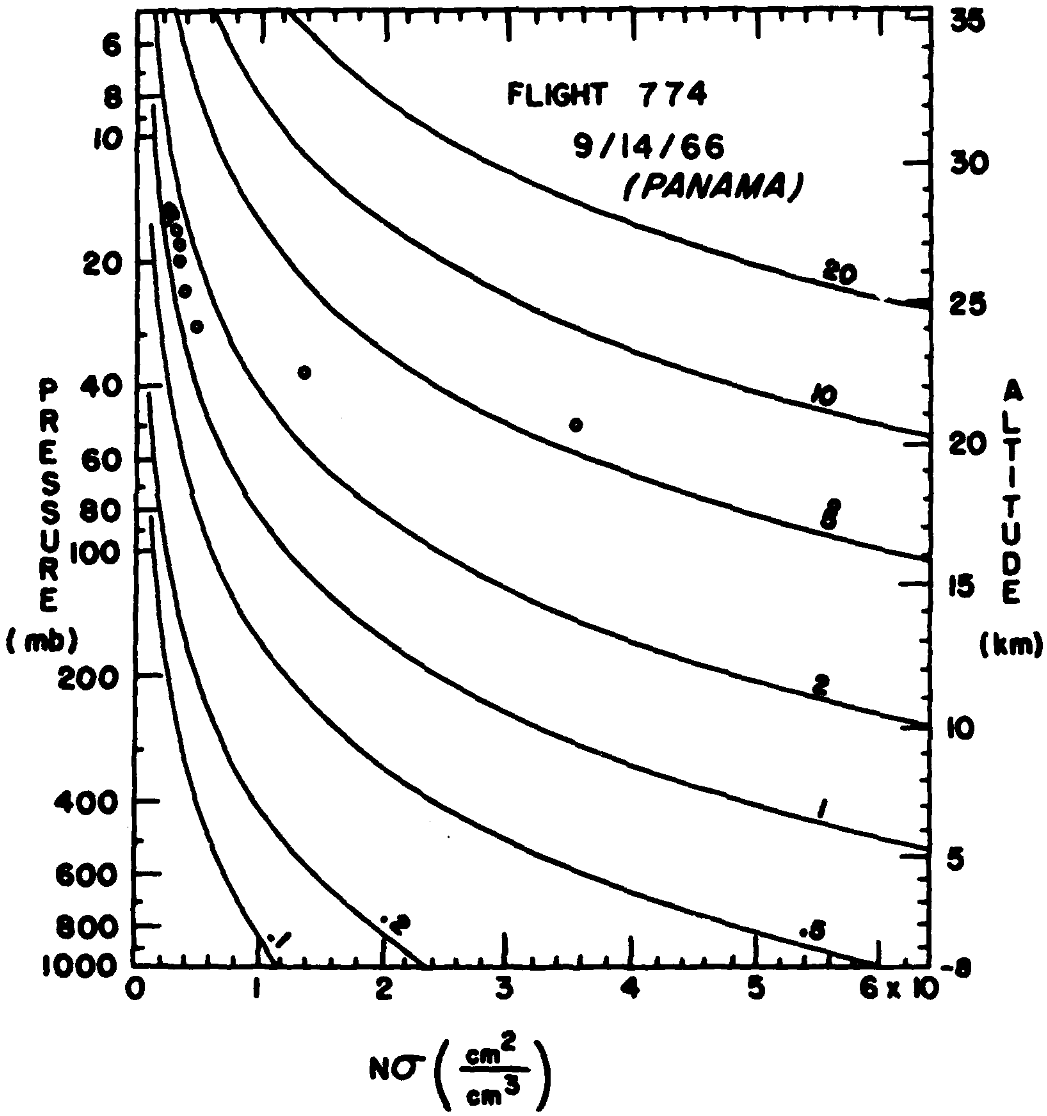
FLIGHT 774
9/14/66
(PANAMA)
PRESSURE (mb)
ALTITUDE (km)
$N\sigma \left(\frac{cm^2}{cm^3}\right)$
6 x 10
20
10
2
1

Figure 16

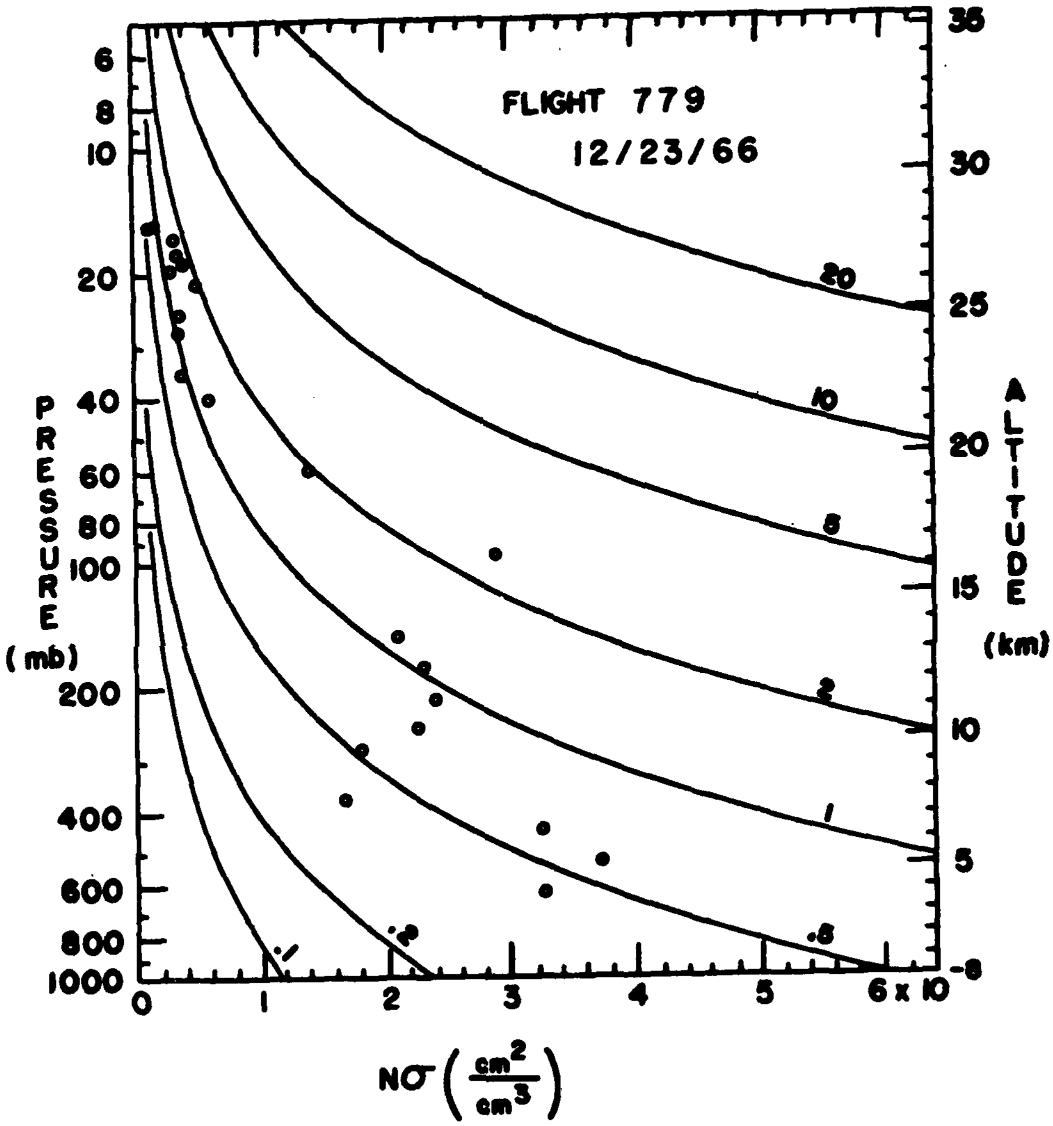

FLIGHT 779
12/23/66
PRESSURE (mb)
ALTITUDE (km)
$N\sigma \left(\frac{cm^2}{cm^3}\right)$
6x10
20
10
5
2
1
.5
.2
.1

Figure 17

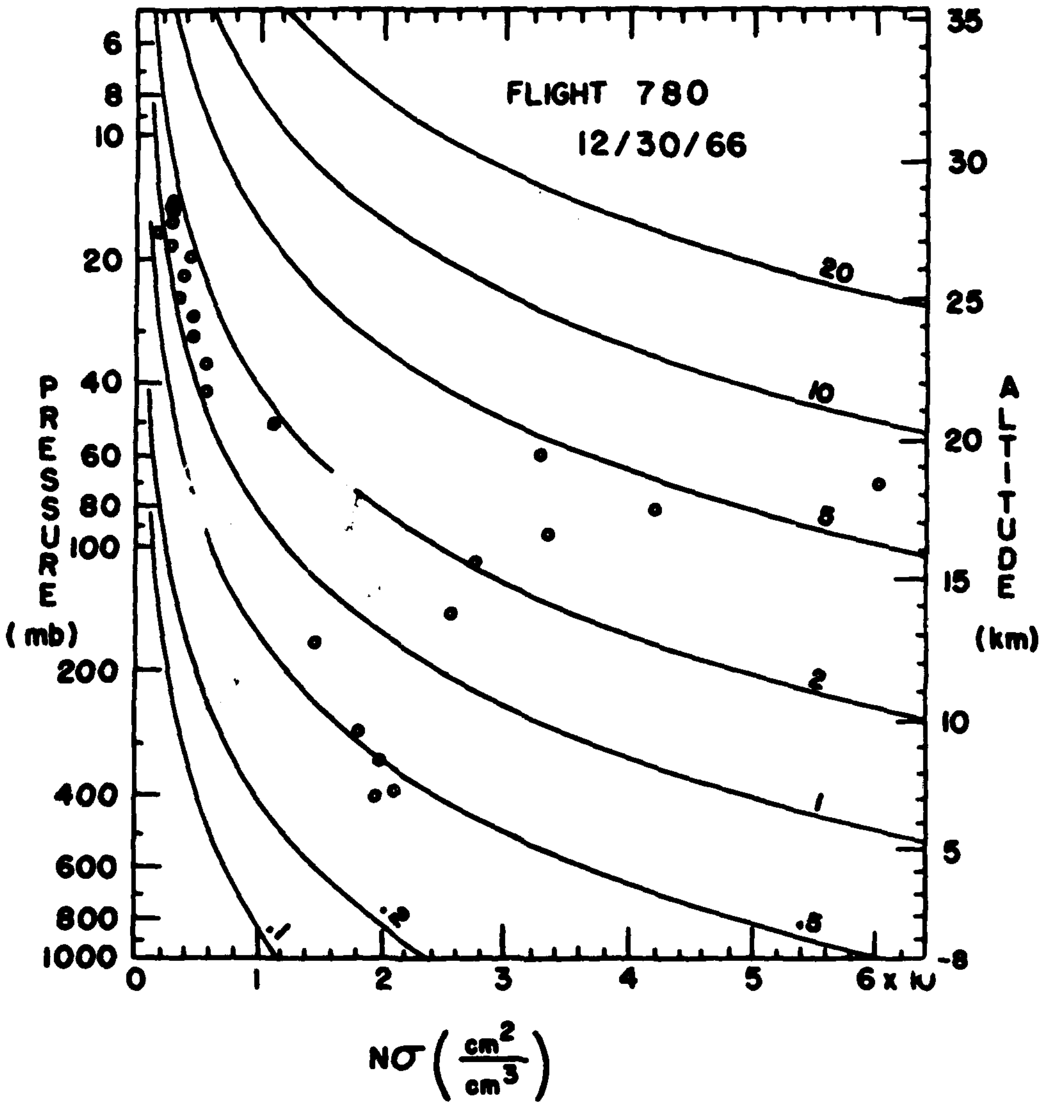

FLIGHT 780
12/30/66
PRESSURE (mb)
ALTITUDE (km)
6
8
10
20
40
60
80
100
200
400
600
800
1000
35
30
25
20
15
10
5
20
10
5
2
1
.5
.2
.1
0
1
2
3
4
5
6 x 10^-8
$N\sigma \left(\frac{cm^2}{cm^3}\right)$

Figure 18

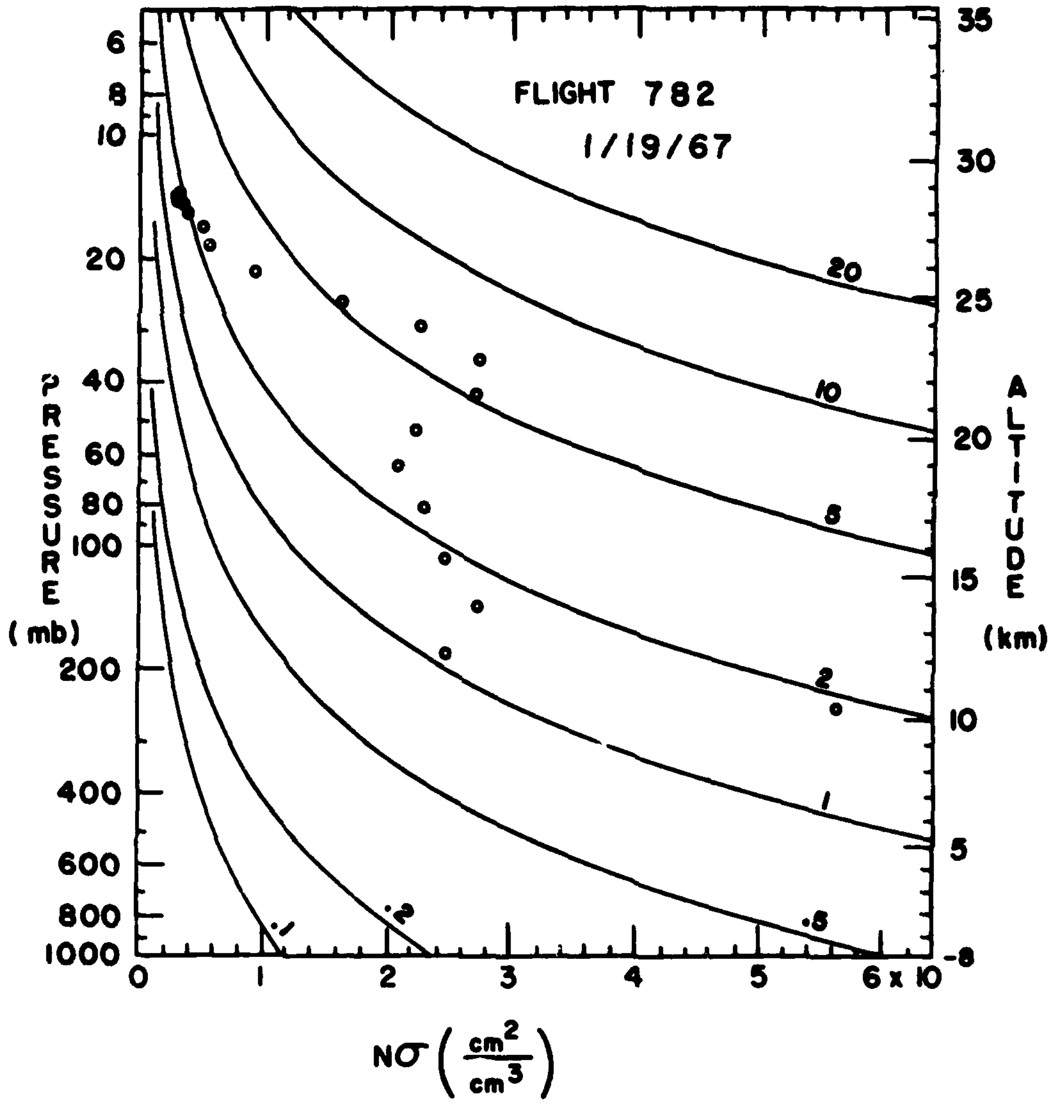
FLIGHT 782
1/19/67
PRESSURE (mb)
ALTITUDE (km)
6
8
10
20
40
60
80
100
200
400
600
800
1000
35
30
25
20
15
10
5
20
10
5
2
1
.5
.2
.1
0
1
2
3
4
5
6 x 10
NO (cm²/cm³)

Figure 19

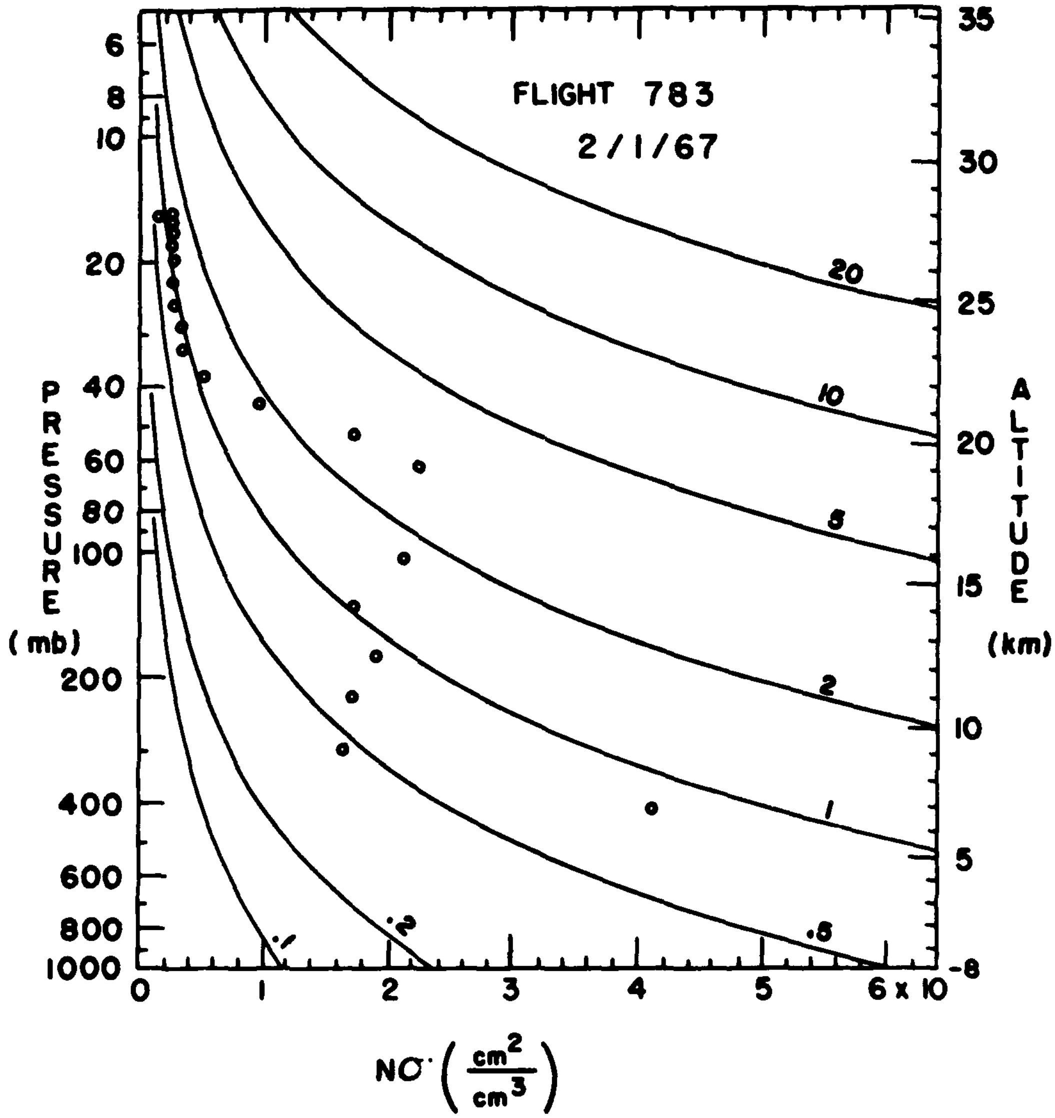

FLIGHT 783
2/1/67
PRESSURE (mb)
ALTITUDE (km)
6
8
10
20
40
60
80
100
200
400
600
800
1000
35
30
25
20
15
10
5
-8
0
1
2
3
4
5
6 x 10
20
10
5
2
1
.5
.2
.1
NO· (cm²/cm³)

Figure 20

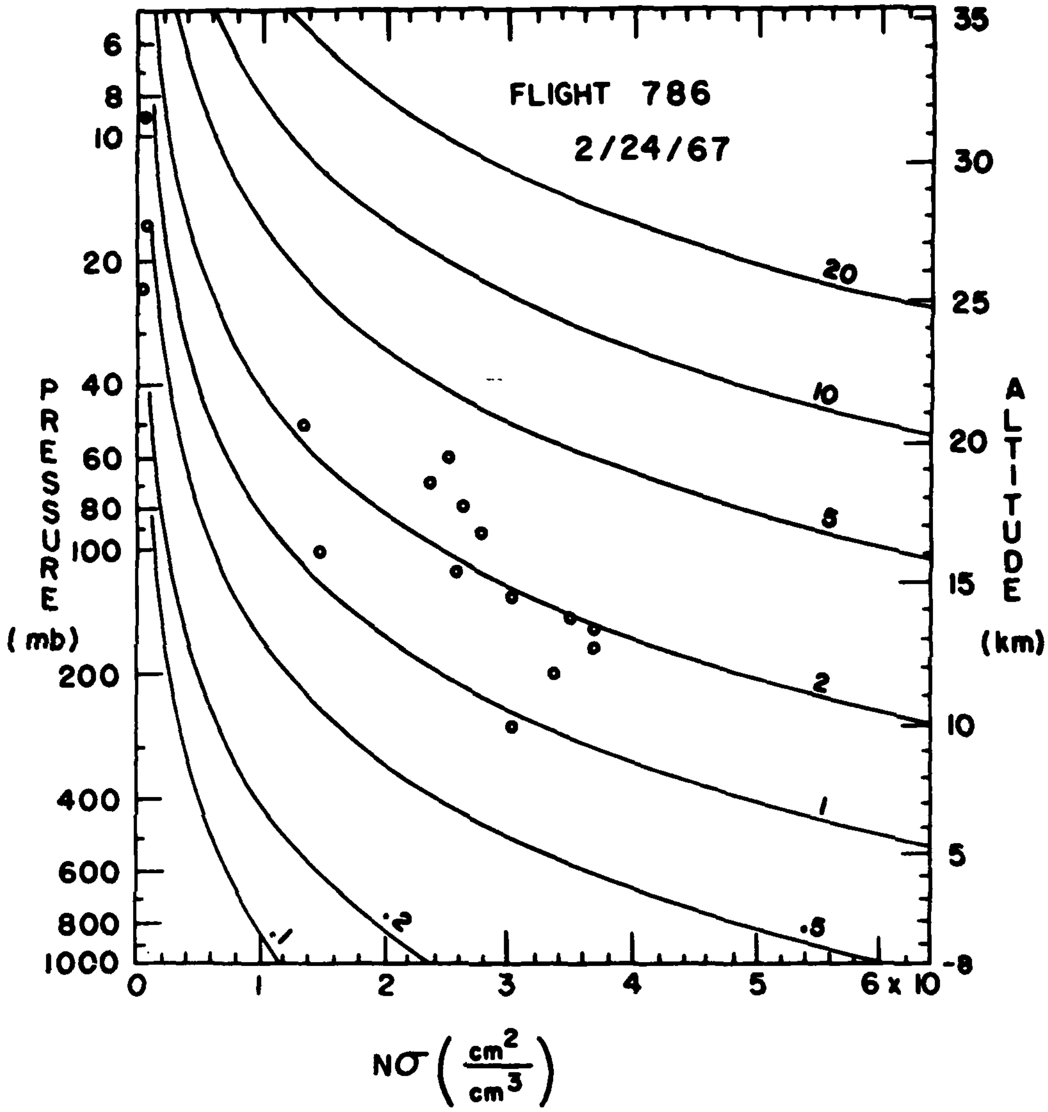
FLIGHT 786
2/24/67
PRESSURE (mb)
ALTITUDE (km)
6
8
10
20
40
60
80
100
200
400
600
800
1000
35
30
25
20
15
10
5
20
10
5
2
1
.5
.2
.1
0
1
2
3
4
5
6 x 10^{-8}
$N\sigma\left(\frac{cm^2}{cm^3}\right)$

Figure 21

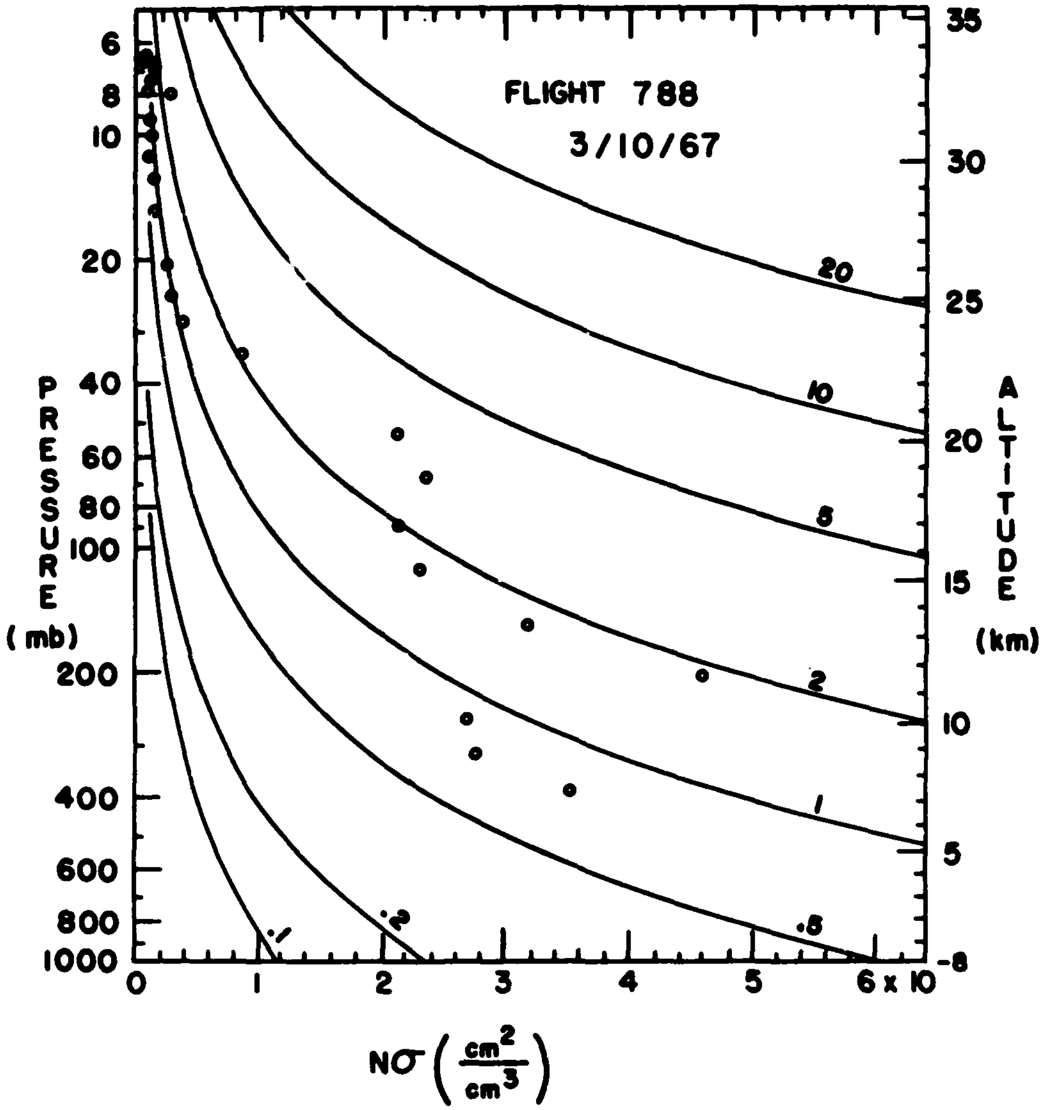

FLIGHT 788
3/10/67
PRESSURE (mb)
ALTITUDE (km)
6
8
10
20
40
60
80
100
200
400
600
800
1000
35
30
25
20
15
10
5
20
10
5
2
1
.5
.2
.1
0
1
2
3
4
5
6 x 10^{-8}
$N\sigma \left(\frac{cm^2}{cm^3} \right)$

Figure 22

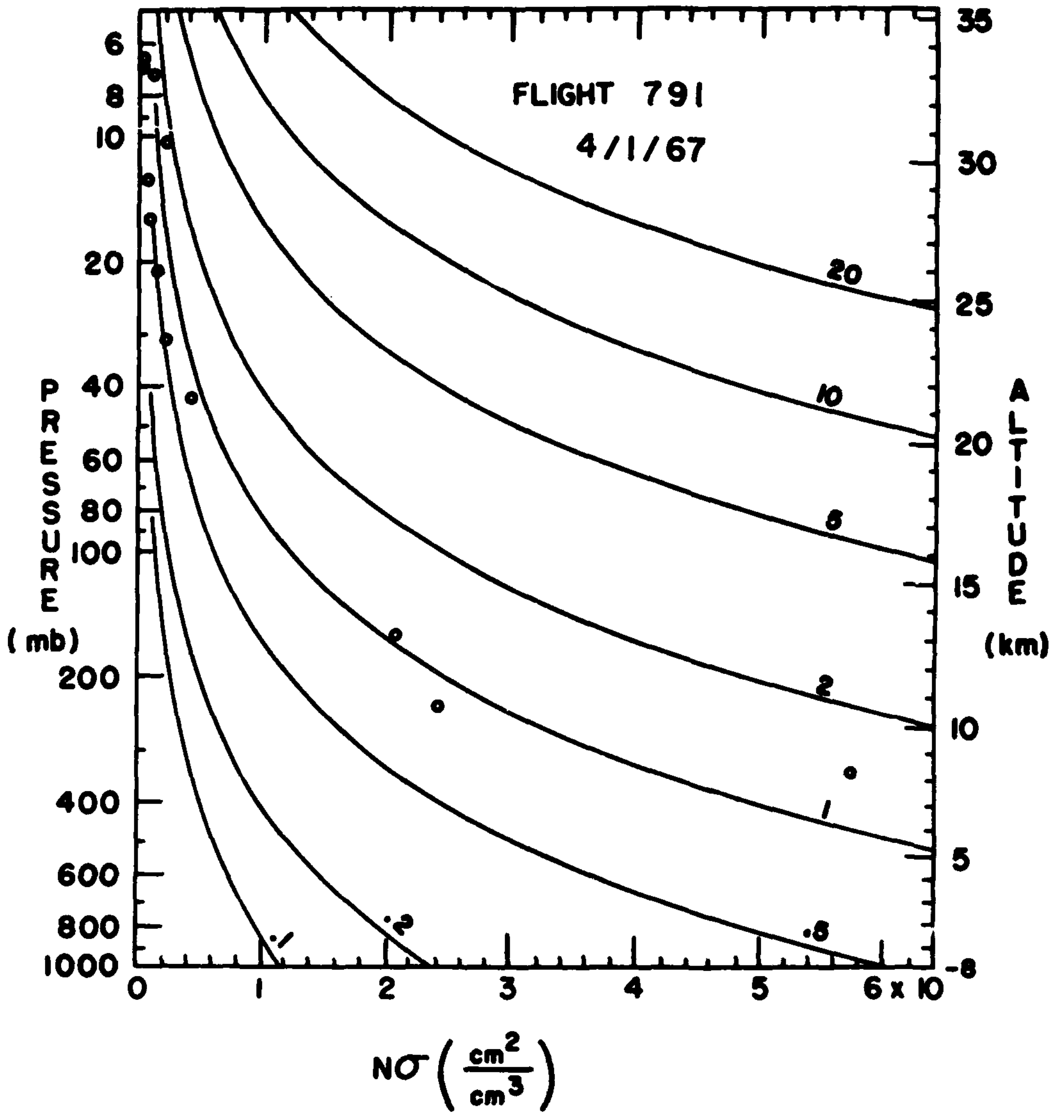

FLIGHT 791
4/1/67
PRESSURE (mb)
ALTITUDE (km)
20
10
5
2
1
.5
.2
.1
6
8
10
20
40
60
80
100
200
400
600
800
1000
35
30
25
20
15
10
5
0
1
2
3
4
5
6 x 10⁻⁸
NO (cm²/cm³)

Figure 23

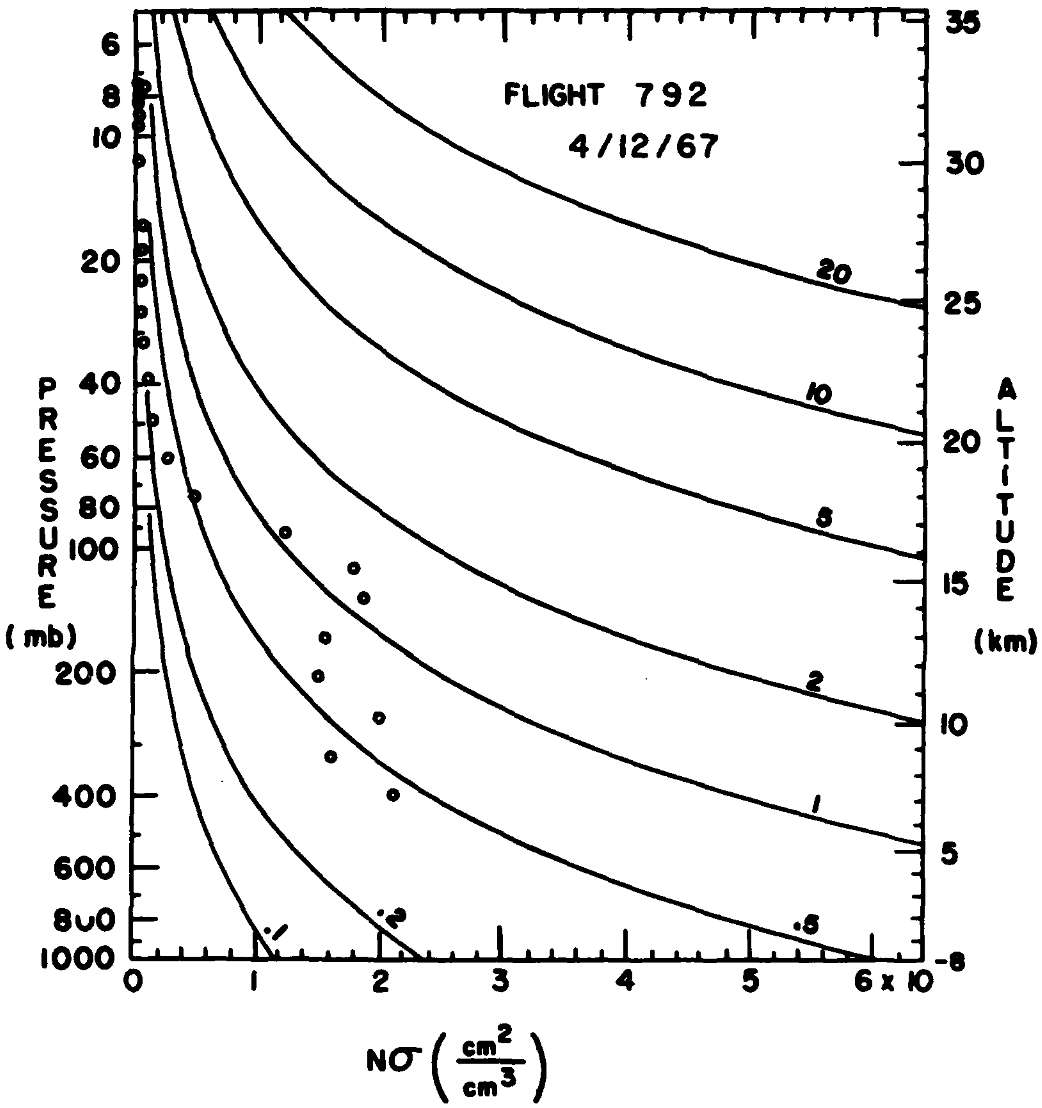
FLIGHT 792
4/12/67
PRESSURE (mb)
ALTITUDE (km)
20
10
5
2
1
.5
.2
.1
6
8
10
20
40
60
80
100
200
400
600
800
1000
35
30
25
20
15
10
5
0
1
2
3
4
5
6 x 10[-8]
$N\sigma \left(\frac{cm^2}{cm^3}\right)$

Figure 24

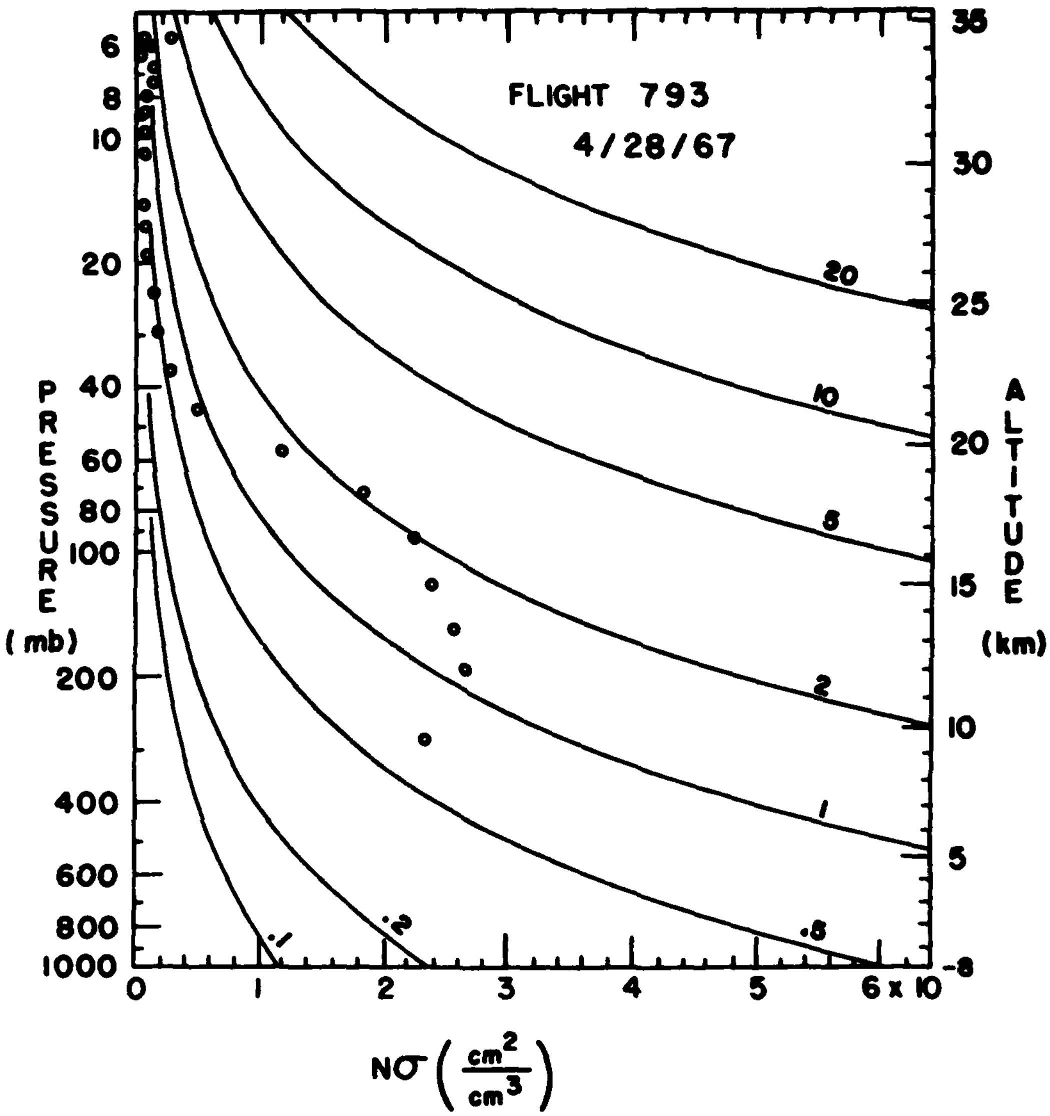

FLIGHT 793
4/28/67
PRESSURE (mb)
ALTITUDE (km)
6
8
10
20
40
60
80
100
200
400
600
800
1000
35
30
25
20
15
10
5
8
0
1
2
3
4
5
6 x 10⁻⁸
20
10
5
2
1
.8
.2
.1
$N\sigma\left(\frac{cm^2}{cm^3}\right)$

Figure 25

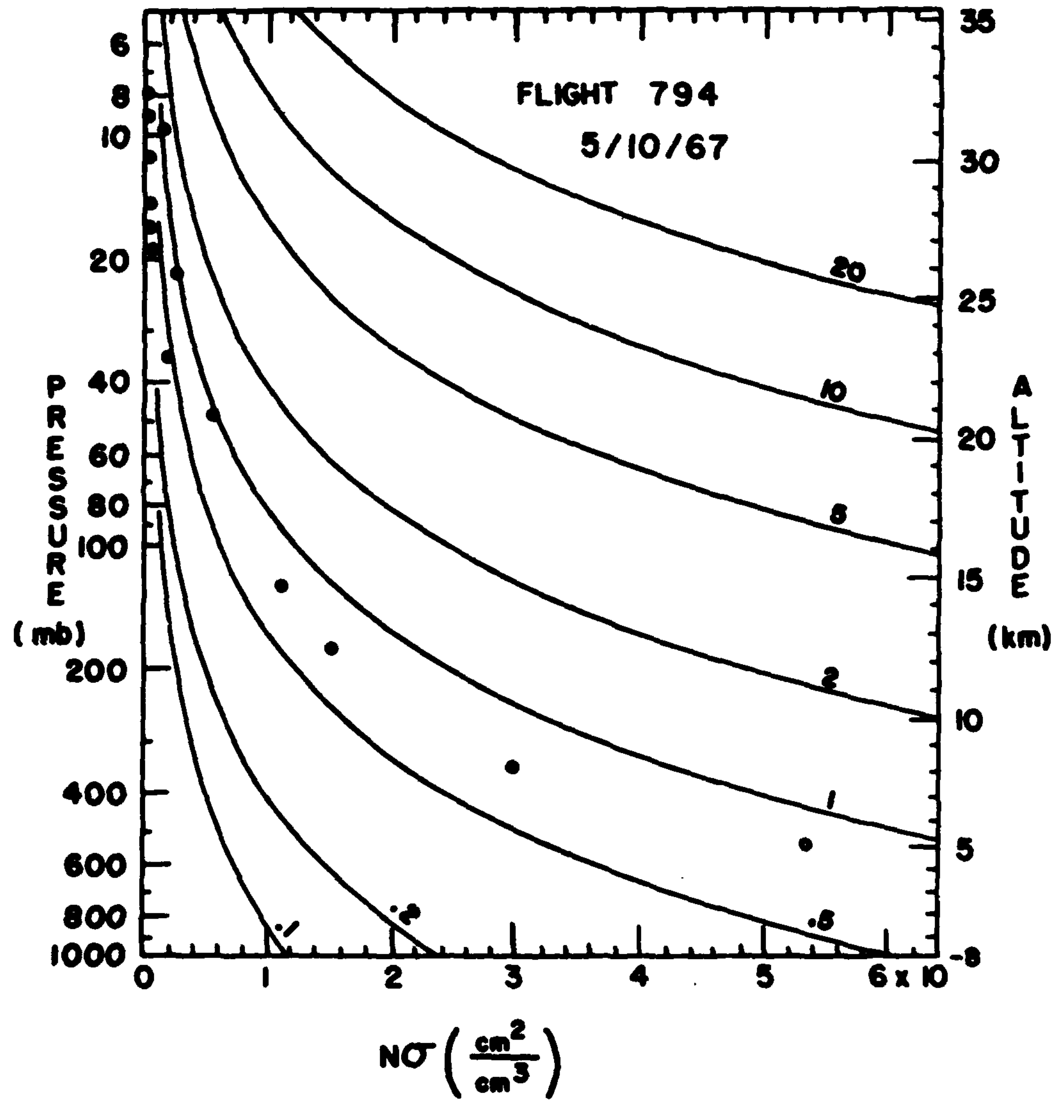
FLIGHT 794
5/10/67
PRESSURE (mb)
6
8
10
20
40
60
80
100
200
400
600
800
1000
ALTITUDE (km)
35
30
25
20
15
10
5
20
10
5
2
1
.5
.2
.1
0
1
2
3
4
5
6 x 10^{-8}
$N\sigma \left(\frac{cm^2}{cm^3}\right)$

Figure 26

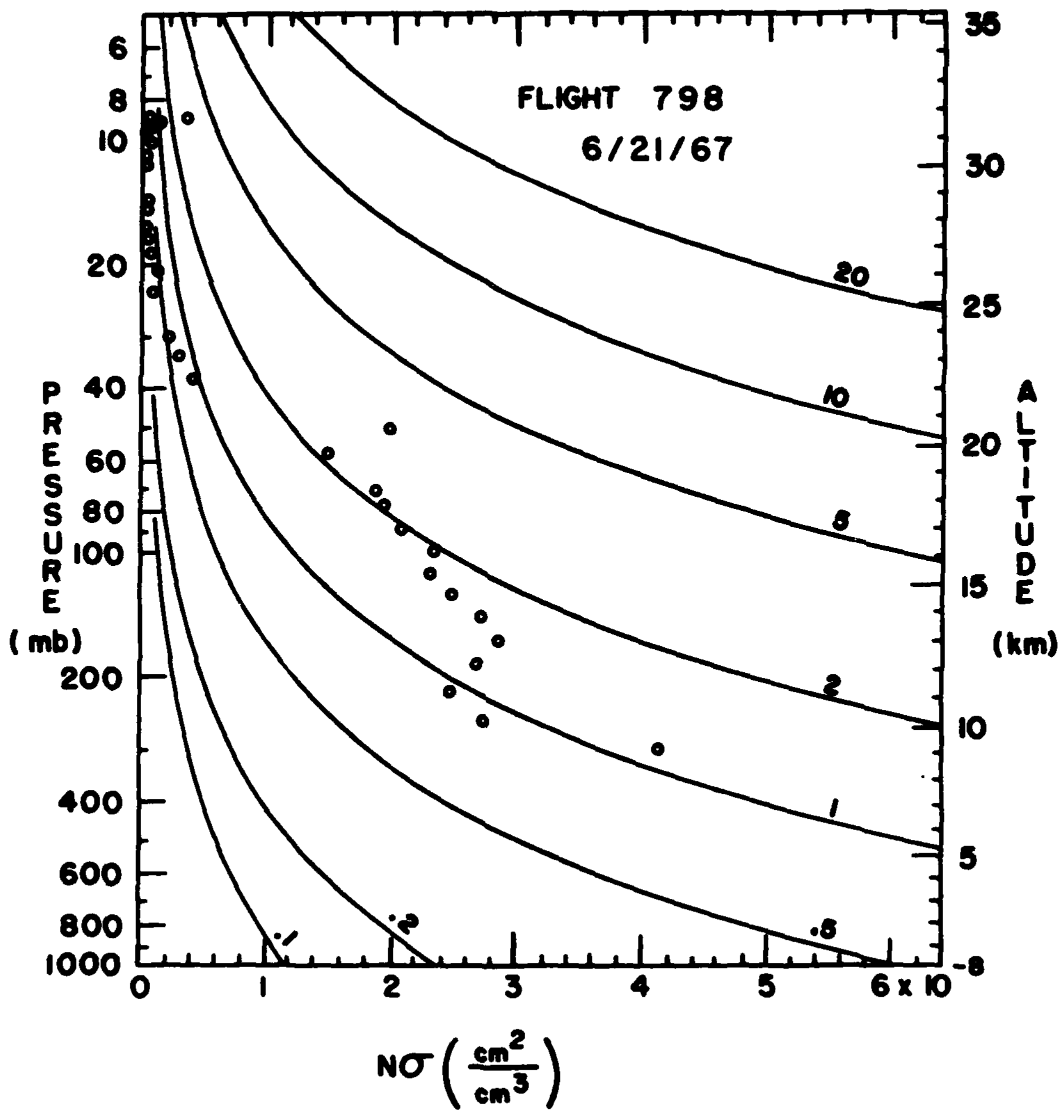
FLIGHT 798
6/21/67
PRESSURE (mb)
6
8
10
20
40
60
80
100
200
400
600
800
1000
ALTITUDE (km)
35
30
25
20
15
10
5
20
10
5
2
1
.5
.2
.1
0
1
2
3
4
5
6 x 10^{-8}
$N\sigma \left(\frac{cm^2}{cm^3}\right)$

Figure 27

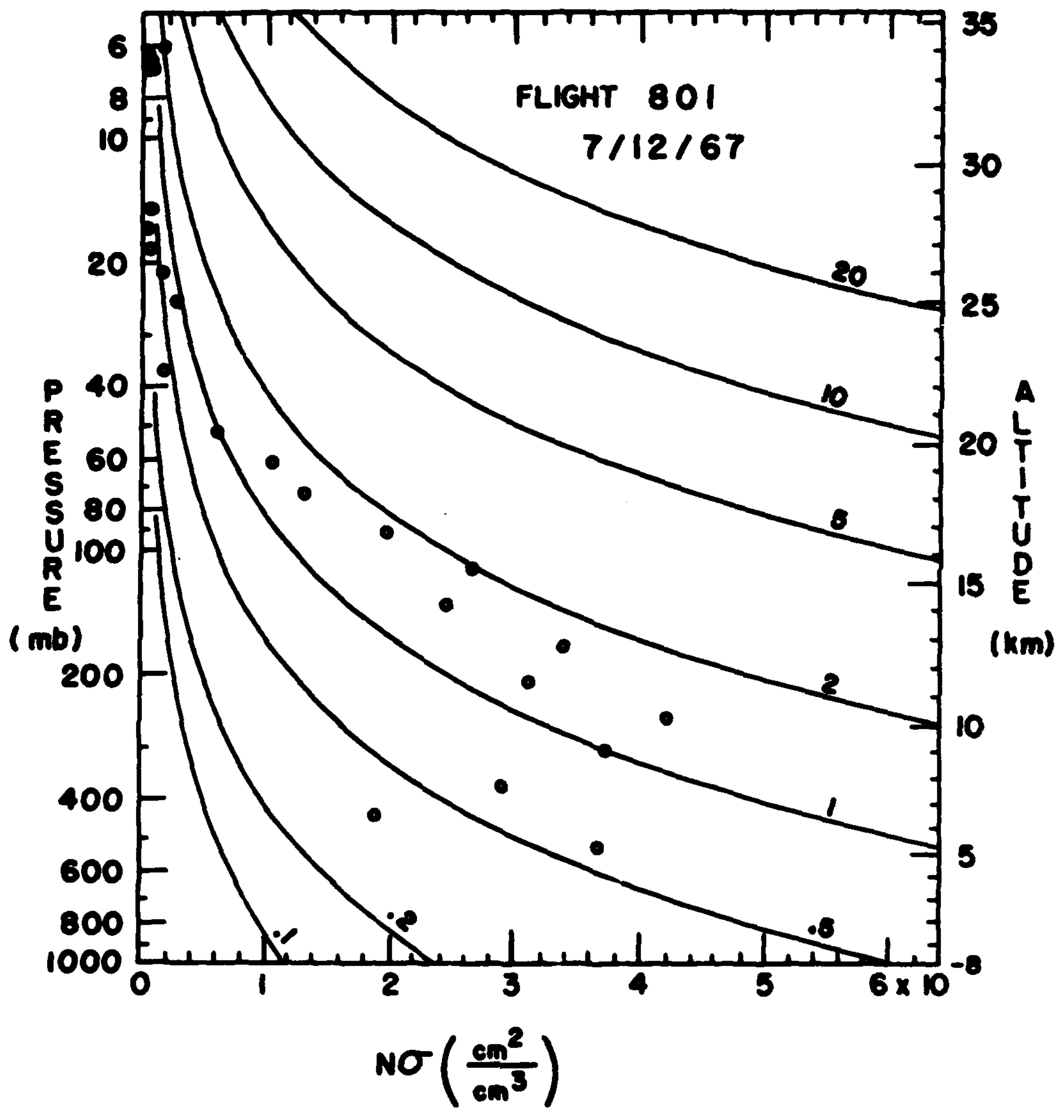
FLIGHT 801
7/12/67
PRESSURE (mb)
ALTITUDE (km)
6
8
10
20
40
60
80
100
200
400
600
800
1000
35
30
25
20
15
10
5
-8
20
10
5
2
1
.5
.2
.1
0
1
2
3
4
5
6 x 10
$N\sigma \left(\frac{cm^2}{cm^3}\right)$

Figure 28

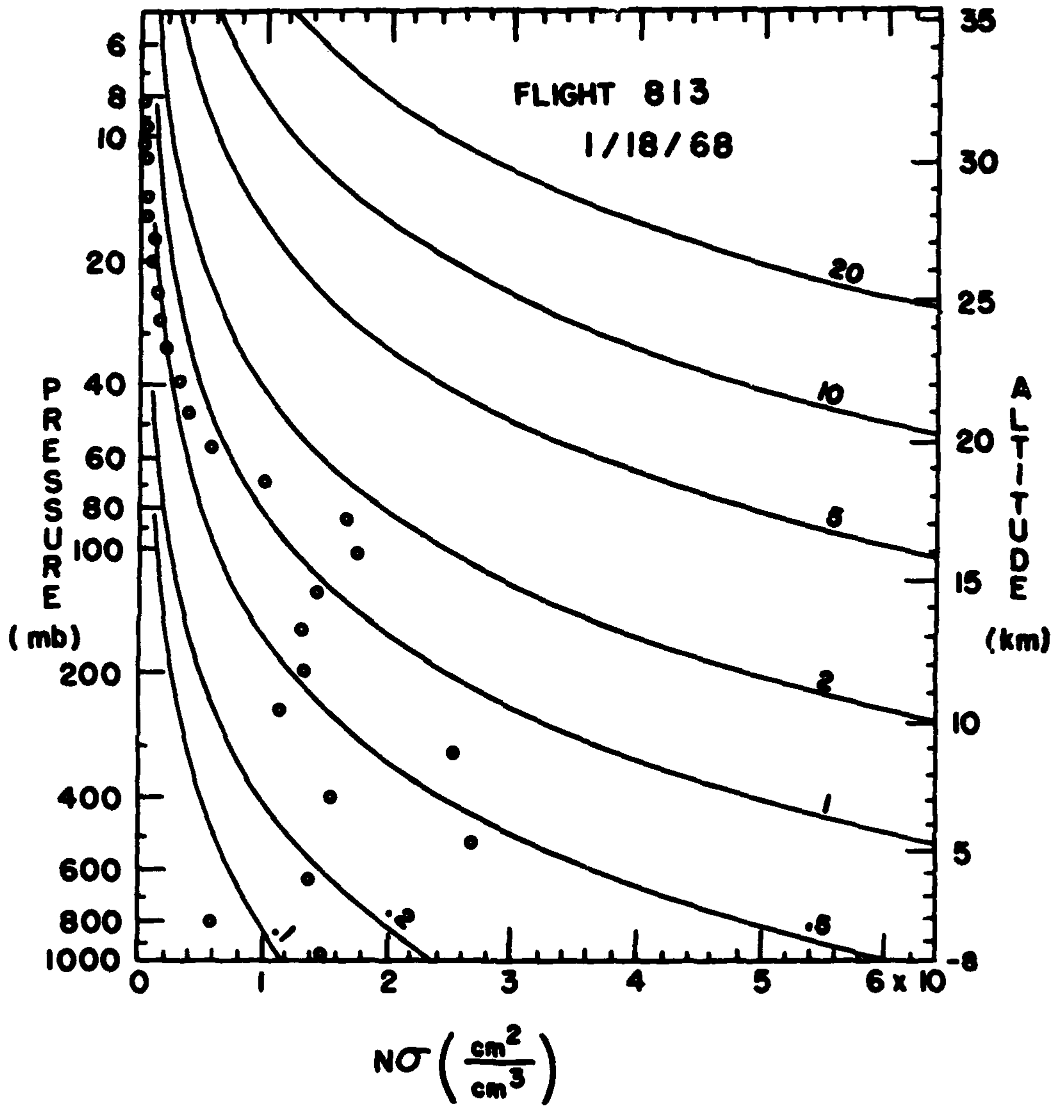

FLIGHT 813
1/18/68
PRESSURE (mb)
6
8
10
20
40
60
80
100
200
400
600
800
1000
ALTITUDE (km)
35
30
25
20
15
10
5
20
10
5
2
1
.5
.2
.1
0
1
2
3
4
5
6 x 10⁻⁸
$N\sigma\left(\frac{cm^2}{cm^3}\right)$

Figure 29

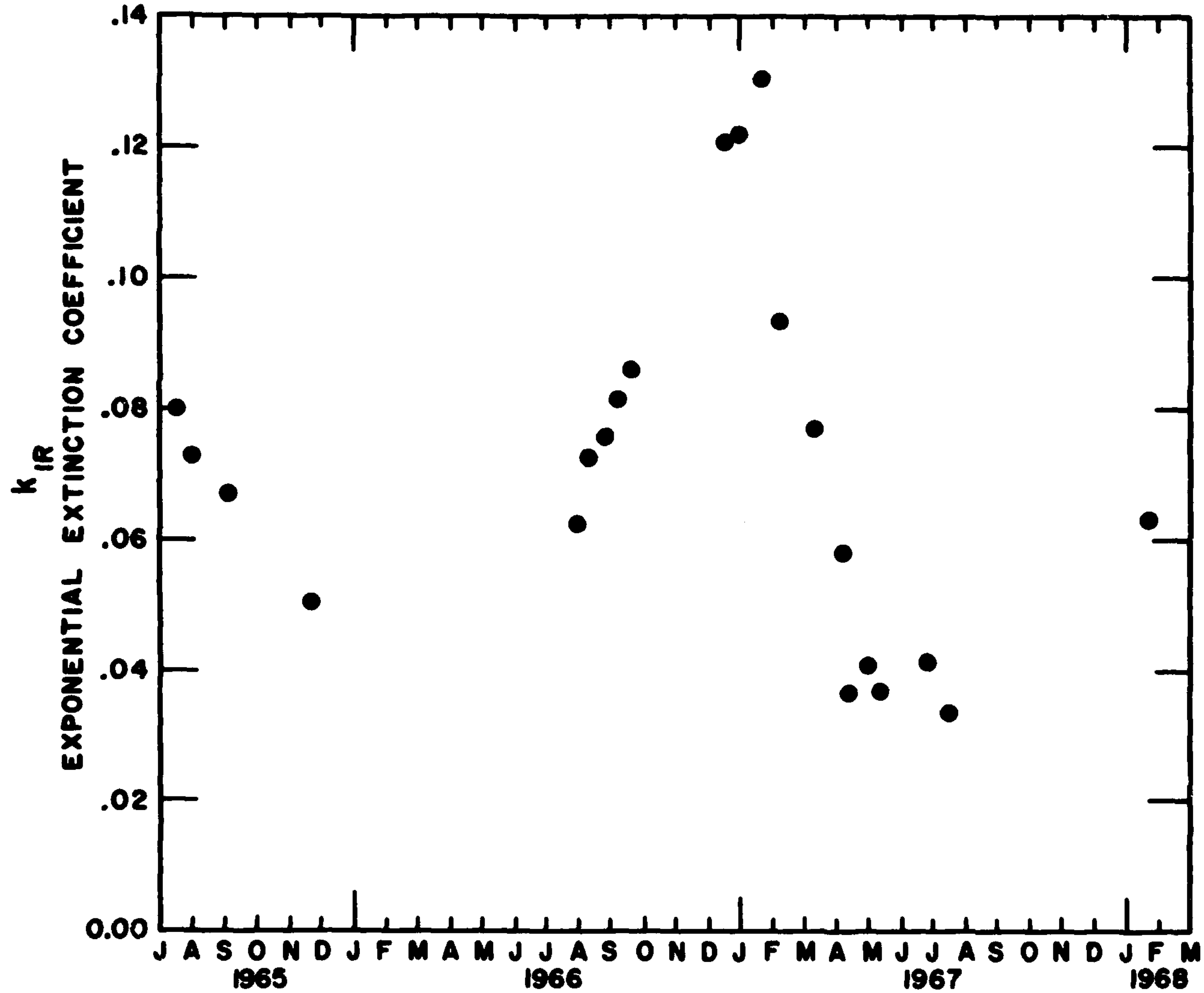
.14
.12
.10
.08
.06
.04
.02
0.00
k_{IR}
EXPONENTIAL EXTINCTION COEFFICIENT
J A S O N D J F M A M J J A S O N D J F M A M J J A S O N D J F M
1965
1966
1967
1968

Figure 30

Security Classification

DOCUMENT CONTROL DATA - R & D

(Security classification of title, body of abstract and indexing annotation must be entered when the overall report is classified)

1. ORIGINATING ACTIVITY (Corporate author) School of Physics and Astronomy University of Minnesota Minneapolis, Minnesota 55455	2a. REPORT SECURITY CLASSIFICATION Unclassified 2b. GROUP

3. REPORT TITLE

The Use of Extinction from High Altitude Balloons as a Probe of the Atmospheric Aerosols.

4. DESCRIPTIVE NOTES (Type of report and inclusive dates)

Atmospheric Physics Technical Report

5. AUTHOR(S) (First name, middle initial, last name)

T. J. Pepin

6. REPORT DATE	7a. TOTAL NO. OF PAGES	7b. NO. OF REFS
October, 1969	41	5
8a. CONTRACT OR GRANT NO. N00014-67-A-0113-0004 b. PROJECT NO. c. d.	9a. ORIGINATOR'S REPORT NUMBER(S) 9b. OTHER REPORT NO(S) (Any other numbers that may be assigned this report)	

10. DISTRIBUTION STATEMENT

Distribution of this document is unlimited.

11. SUPPLEMENTARY NOTES	12. SPONSORING MILITARY ACTIVITY
	Office of Naval Research Department of the Navy Washington, D. C. 20546

13. ABSTRACT

A simple instrument is described that measures the intensity of solar radiation in four spectral regions. Instruments of this type have been used to observe the atmospheric extinction from high altitude balloons at sunrise since mid 1965. The data from these balloon flights are described and the vertical profiles of atmospheric aerosols determined from these measurements are presented. Evidence is given for the time variation of aerosols at high altitude.